





RESEARCH ARTICLE

# Climatic factors affecting Kamchatka glacier recession

I. A. Korneva<sup>1</sup>  | P. A. Toropov<sup>1,2</sup>  | A. Ya. Muraviev<sup>1</sup>  | M. A. Aleshina<sup>3</sup> 

<sup>1</sup>Glaciology Department, Institute of Geography of the Russian Academy of Sciences, Moscow, Russia

<sup>2</sup>Department of Meteorology and Climatology, Faculty of Geography, Moscow State University, Moscow, Russia

<sup>3</sup>Laboratory of Climatology, Institute of Geography of the Russian Academy of Sciences, Moscow, Russia

## Correspondence

I. A. Korneva, Glaciology Department, Institute of Geography of the Russian Academy of Sciences, Moscow, Russia.  
Email: [comissa@mail.ru](mailto:comissa@mail.ru)

## Funding information

Research Plan of the Institute of Geography RAS, Grant/Award Number: FMGE-2019-0004; Russian Science Foundation, Grant/Award Number: 22-17-00159

## Abstract

The reduction in the area and volume of glaciation in all mountain regions of the Earth has strongly accelerated for the last decades. In this work, we analysed the trends of the main climatic parameters which caused the glacier recession in the Kamchatka Peninsula. It was shown that the glaciers of the northern part of the Sredinny Range decreased by 125 km<sup>2</sup> (35.6%) from 1950 to 2016–2017. The average rate of their reduction in the period from 2002 to 2016–2017 (1.45%/year) increased approximately 4.3 times compared to the period 1950–2002 (0.34%/year). The greatest reduction is observed in small glaciers with an area of less than 0.1 km<sup>2</sup> and in glaciers with southeastern and southern expositions. On the Kronotsky Peninsula, the glacier area reduction for 1957–2019 was equal to 32.1 km<sup>2</sup> (35.6%), and the rates were almost the same in the periods of 1957–2000 (0.61%/year) and 2000–2019 (0.67%/year). According to the data of weather stations and ERA5 reanalysis, it was shown that, in the ablation (summer) period the warming rate was minimal (0.3°C/10 years) and in the accumulation period a significant decrease in precipitation (5%–10%/10 years) was revealed in some areas. At the same time, a significant increase in the radiation balance was revealed in the warm season along with a tendency in downward shortwave radiation increase for the last two decades due to a decrease in cloud amount. These trends are in good agreement with the growth of the geopotential height over the North Pacific during the warm season in the 21st century, and with the growth of velocity divergence in the middle troposphere and the intensification of downward air movements. All this confirms an increase in anticyclone frequency in the warm season, which could be the cause of a radiation balance increase and, consequently, an increase in glacier ablation.

## KEYWORDS

ablation, climatic factors, glacier recession, Kamchatka glaciers, radiation balance

## 1 | INTRODUCTION

The reduction in the area and volume of glaciation in all mountain regions of the Earth started in the 1980s and for the last 15–20 years on average over the globe was equal to –1.5%/year (Hock et al., 2019), which can be

considered catastrophic. At first sight, such intense deglaciation is one of the responses to modern global warming: numerous studies in the 21st century showed a noticeable mean annual air temperature increase in the high mountain regions of the Earth (Pepin et al., 2022). For example, in the Mountains of Tibet, the air temperature

increased by 0.3–0.4°C for the years 1980–2010 (You et al., 2010). In the Alps, the air temperature trend over the 20th century was equal to +0.14°C/10 years (Gilbert & Vincent, 2013), and this value hasn't changed in the 21st century (Rottler et al., 2019).

However, as it can be seen from different studies the air temperature rise is not always the main reason for glacier recession. For example, in the high mountainous regions of the Caucasus, the positive air temperature trend in the warm season is statistically insignificant (Toropov et al., 2019), while the negative trend in the glaciation area reaches 1.5%/year (Tielidze & Wheate, 2018), exceeding the global average (Hock et al., 2019). It is assumed that the main trigger for the Caucasus glaciers reduction is the increase of incoming shortwave radiation associated with the negative trend of cloud cover. The decrease in cloud cover is linked with an increase in the frequency of anticyclones in the region, which may be one of the consequences of the Hadley Cell Expansion to the north (Lu et al., 2007). Some researchers attribute the air temperature rise and glacier recession in the Alps to an increase in the frequency of anticyclones (Rottler et al., 2019). On the contrary, an incoming shortwave radiation increase in the mountain-glacial regions of the Earth (for example, in the Alps) can be associated with a global decrease in the aerosol optical thickness of the atmosphere (Norris & Wild, 2007; Philipona, 2013; Philipona et al., 2009).

Another effective mechanism for the glacier recession through the summer mass balance is a surface albedo decrease due to a reduction in snow cover extent and duration, the dust storms frequency increase (Di Mauro et al., 2019; Dumont et al., 2020) and black carbon deposition (Ginot et al., 2014). In addition, a significant factor for melting acceleration may be an increase in downward long-wave radiation, both due to carbon-containing greenhouse gases concentration increase, and an increase in atmospheric moisture content due to heat content growth (Philipona et al., 2005). In addition, in some regions, a more active melting of mountain glaciers may be associated with an increase in Foehns frequency, when the turbulent heat exchange between air and the ice surface is very intense (Elvidge et al., 2020; Shestakova et al., 2022). Finally, the area of mountain glaciation may decrease due to winter precipitation decline – this effect is clearly observed for example in the Caucasus (Toropov et al., 2019).

Despite Kamchatka being the second largest mountain-glacier region in Russia (after the Caucasus), the climate and glaciation of the region are poorly explored due to rather severe climatic conditions and the large distance from major economic cities. A good overview of the glacier dynamics in Kamchatka in response to changing air temperature and precipitation is given in Fukumoto et al. (2023). However, the analysis

presented in that article covers only the period 2000–2016. There was no detailed comparison with the variations in the 20th century, as well as an extensive analysis of the climatic and atmospheric circulation effects on the glacier reduction. The main goal of our work is to identify trends in basic glaciological characteristics for the two large mountain–glacier regions of Kamchatka – the northern part of the Sredinny Range and the Kronotsky Peninsula. These areas of glaciation in Kamchatka are not influenced by modern volcanism (Muraviev, 2020b), therefore they are suitable for investigating the response of glaciers to climate change. In this article, we analyse the trends in glaciation total area from the middle of the 20th century to the present and their altitudinal distribution. At the same time, the main climatic parameter changes are estimated by weather stations and reanalysis data and are compared with the glacier area trends. In the final part of the work the main conclusions about the causes of Kamchatka climate change and consequently, the glacier area changes are made, based on the analysis of large-scale atmospheric circulation over the Pacific region and the eastern part of Northern Eurasia.

## 2 | RESEARCH AREA

Kamchatka is a large peninsula located in the east of Russia between 52–62 degrees north latitude and 155–163 degrees east longitude, stretching in the meridional direction for about 1200 km. More than three-fourths of Kamchatka are mountain areas and the unique feature of the peninsula is an extremely high concentration of active volcanoes (currently 29) (Fedotov & Masurenkov, 1991). The highest point of the peninsula and the Asian part of Russia is the Klyuchevskoy volcano (about 4750 m), which is covered with significant glaciation.

According to the latest data, there are 732 mountain glaciers in Kamchatka with a total area of  $682.8 \pm 29.0 \text{ km}^2$  (Khromova et al., 2021). The largest areas of glaciation in Kamchatka are the northern part of the Sredinny Range (465 glaciers with a total area of  $255 \pm 15 \text{ km}^2$  (Muraviev, 2020a)) and the Klyuchevskaya group of volcanoes (40 glaciers with a total area of  $214.3 \pm 6.6 \text{ km}^2$  (Muraviev, 2020b)). Cirque and cirque-valley glaciers predominate, while the largest areas are occupied by cross-valley and cirque-valley glaciers (Muraviev, 2020b). Morphological types of glaciers specific to volcanic structures (barrancos, caldera-valley, crater, etc.) are common in Kamchatka.

The glaciation of areas of active volcanism in Kamchatka, such as the Klyuchevskaya and Avachinskaya groups of

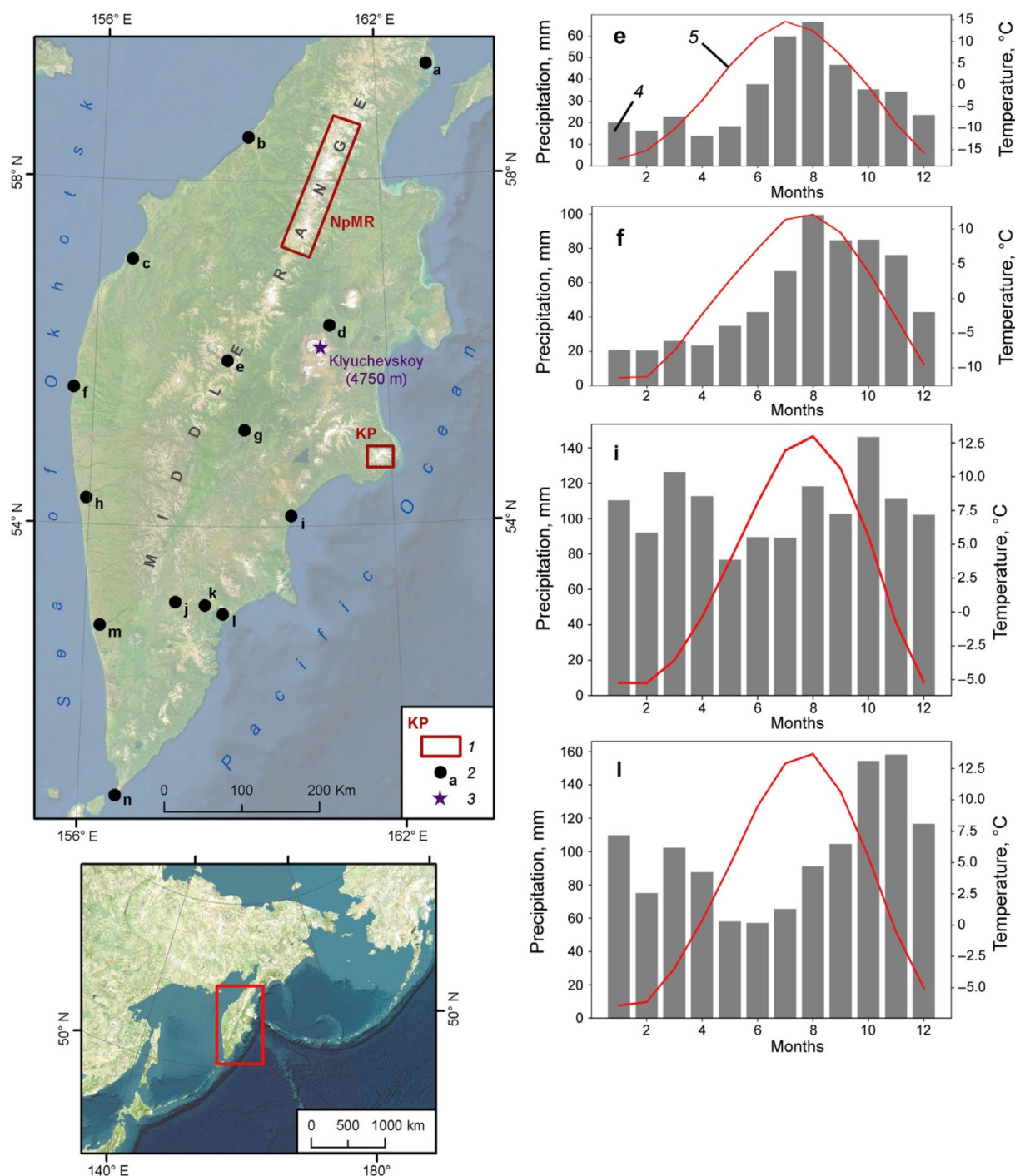


**FIGURE 1** Research Area (Kamchatka Peninsula) and climate diagrams at the individual weather stations; 1 – the location of the Northern part of Sredinniy Ridge (NpMR) and Kronotsky Peninsula (KP): the glaciation, analysed in this paper, is located within these areas; 2 – weather stations: (a) Ossora, (b) Ust-Voiampolka, (c) Ust-Khayryuzovo, (d) Kluchi, (e) Esso, (f) Icha, (g) Dolinovka, (h) Sobolevo, (i) Semyachik, (j) Nachiki, (k) Sosnovka, (l) Petropavlovsk-Kamchatsky, (m) Bolsheretsk, (n) Mys Lopatka; 3 – volcanoes; 4 – precipitation; 5 – air temperature. [Colour figure can be viewed at [wileyonlinelibrary.com](https://onlinelibrary.wiley.com)]

volcanoes, is currently not shrinking (Khromova et al., 2019; Muraviev & Muraviev, 2016). This is primarily due to the thick surface moraine of volcanic origin covered the glaciers surface in these regions, which significantly reduces surface ablation. Therefore, the dynamics of glaciers located on active volcanoes cannot be used as an

indicator of climate change. Fluctuations of such glaciers are primarily determined by volcanic activity, which often exceeds the climatic factor of the glaciers existence (Muraviev, 2017).

The main factors that forms the Kamchatka climate are very intense cyclonic activity (Brief description..., 2020) and

the cold sea surface (the Kuril Current in the east and the Sea of Okhotsk in the west). The radiation balance and air temperature are characterized by pronounced seasonality: the annual temperature amplitude on the sea coasts is 15–20°C and in the interior and northeastern regions of the peninsula it sometimes reaches 30°C (Figure 1), corresponding to continental climate. In general, Kamchatka climate has monsoon features: winter is characterized by northwestern winds blowing along the eastern edge of the Asian anticyclone, and summer – by southeastern winds blowing from the ocean driving by North Pacific High and the low-pressure system over Southeast Asia (Lozhkin & Shevchenko, 2021). Therefore, in general, most regions of Kamchatka are characterized by a summer–autumn maximum of precipitation (Figure 1). This feature is broken on the Pacific coast of the peninsula, where the annual precipitation pattern looks more uniform (with weakly pronounced maxima in spring and autumn – Figure 1, weather stations ‘i’ and ‘l’). This is due to the extremely intense cyclonic activity over the Pacific Ocean in winter: in total, up to 100 cyclones can be observed during the cold season in Kamchatka (Shkaberda & Vasilevskaya, 2014). The influence of dry cold air from Siberia can be visible already 100–150 km to the west of the coast, where winter precipitation significantly decreases (Figure 1, weather station ‘e’). In general, the peninsula belongs to the zone of excessive moisture, where the annual precipitation significantly exceeds the annual evaporation. Therefore, the plains and valleys of the peninsula are characterized by waterlogged soils and swampiness, and the glaciation in the mountain regions. The maximum annual precipitation (similar to the humid subtropics – about 2000 mm) falls on the windward slopes of the ridges of the southern volcanic region, as well as in the central part of the Kronotsky Peninsula (Kondratyuk, 1974). The minimum (400 mm) precipitation falls in the north of the peninsula in the central part of the Kamchatka River valley. In other parts of the peninsula precipitation varies from 1500 mm in the eastern mountain volcanic region to 500 mm on the northwestern coast. Kamchatka's climate unique feature is a thick snow cover, its average depth is one of the highest on Earth – about 1.5 m. In general, snow cover increases from the northwest (about 0.5 m) to the east and southeast (up to 2.5 m) and from the coasts to the mountains.

### 3 | DATA

#### 3.1 | Glaciological data

The following data were used to assess the glaciation changes in the studied areas: (1) results of the investigation of glaciation changes in the northern part of the Sredinny Range for the periods from the year 1950 to 2016–

2017, 1950–2002 and from the year 2002 to 2016–2017 (Muraviev, 2020a); (2) Sentinel-2 satellite image of L1C processing level dated 12 September 2019 with a spatial resolution of 10 m for Kronotsky Peninsula; (3) Landsat-7 satellite image of L1TP processing level dated 9 June 2000 for Kronotsky Peninsula; (4) digital elevation model mosaic (hereinafter – DEM) ArcticDEM v3.0 (Porter et al., 2018) with a spatial resolution of 2 m; (5) DEM ASTER GDEM V3 (NASA/METI/AIST/Japan Space Systems & U.S./Japan ASTER Science Team, 2018) with a spatial resolution of 30 m in the geographic coordinate system on the WGS 1984 ellipsoid; (6) data from the Catalogue of Glaciers of the USSR (Vinogradov, 1968).

Information on the glacier boundary's location in the northern part of the Sredinny Range in 2016–2017 (Muraviev, 2020a) was obtained as a result of processing data from the glacier boundaries interpretation on satellite images of Sentinel-2 (with spatial resolution 10 m) dated 19 August 2016, 10 September 2017 and 31 August 2018 (Table 1). At the same time, 43.1% of the total number of glaciers were processed using four images dated 19 August 2016; 53.4% – based on four images dated 10 September 2017; 3.4% – based on two images dated 31 August 2018. The area of glaciers, whose boundaries were interpreted from images dated 31 August 2018, is only 1.3% of the total glaciation area. Based on this we can conclude that the results of this work reflect the glaciation parameters of the northern part of the Sredinny Range in 2016–2017.

Initial data on the glacier boundary's location in the northern part of the Sredinny Ridge in 2002 were taken from Muraviev and Nosenko (2013). They were obtained as a result of manual interpretation of four ASTER satellite images (orthoproduct) dated 18 August 2002 with a spatial resolution of 15 m (Table 1). The original data files in the vector format ‘shapefile’ (polygonal) were analysed after correcting the three glaciers' boundaries positions. It should be noted that the spatial coverage of the northern part of the study area by the 2016–2017 Sentinel-2 images slightly exceeds its coverage by the 2002 ASTER images used (Muraviev, 2020a, 2020b; Muraviev & Nosenko, 2013), and its coverage by the schemes used in Glacier Catalogue (Vinogradov, 1968). The spatial coverage reflecting the glaciation parameters of the northern part of the Sredinny Range in 2016–2017 and the Kronotsky Peninsula in the year 2019 was included in the Catalogue of Russian Glaciers (Glaciers-of-russia-english/main-page, 2022; Khromova et al., 2021).

#### 3.2 | Meteorological data

The main climate data used in this work were the data from 15 network weather stations of the Kamchatka



TABLE 1 Satellite images are used in this work.

Satellite	Survey date	Satellite image identificator (ID)	
The northern part of the Sredinny Range			
Sentinel-2	19.08.2016	S2A_OPER_MSI_L1C_TL_SGS__20160819T005149_20160819T023316_A006048_T57VWD_N02_04_01	
		S2A_OPER_MSI_L1C_TL_SGS__20160819T005149_20160819T023316_A006048_T57VWE_N02_04_01	
		S2A_OPER_MSI_L1C_TL_SGS__20160819T005149_20160819T023316_A006048_T57VXE_N02_04_01	
		S2A_OPER_MSI_L1C_TL_SGS__20160819T005149_20160819T023316_A006048_T57VXF_N02_04_01	
	10.09.2017	L1C_T57VWD_A011582_20170910T003603	
		L1C_T57VWE_A011582_20170910T003603	
		L1C_T57VXE_A011582_20170910T003603	
		L1C_T57VXF_A011582_20170910T003603	
	31.08.2018	L1C_T57VWD_A007750_20180831T003556	
		L1C_T57VWE_A007750_20180831T003556	
	ASTER	18.08.2002	AST14DMO_00308182002003918_20100420061734_1343
			AST14DMO_00308182002003900_20100420061734_1350
AST14DMO_00308182002003926_20100420061734_1371			
AST14DMO_00308182002003909_20100420061734_1373			
Kronotsky Peninsula			
Sentinel-2	12.09.2019	L1C_T57UXA_A013141_20190912T002608	
Landsat-7	06.09.2000	LE07_L1TP_098022_20000906_20170210_01_T1	

TABLE 2 Weather stations in the Kamchatka Peninsula were used in this work.

WMO station number	Station name	Latitude °N	Longitude °E	Height, m	Time period
32213	Mys Lopatka	50°52'	156°41'	48	1966–2020
32246	Ossora	59°18'	163°10'	3	1966–2020
32252	Ust-Voiampolka	58°30'	159°10'	4	1936–2020
32287	Ust-Khayryuzovo	57°05'	156°42'	5	1932–2020
32363	Esso	55°55'	158°43'	480	1941–2020
32389	Kluchi	56°19'	160°50'	28	1914–2020
32411	Icha	55°35'	155°35'	8	1936–2020
32447	Dolinovka	55°07'	159°04'	101	1966–2020
32477	Sobolevo	54°18'	155°56'	13	1937–2020
32509	Semyachik	54°07'	159°59'	28	1936–2020
32539	Nachiki	53°07'	157°44'	315	1935–2020
32547	Sosnovka	53°05'	158°18'	40	1966–2020
32562	Bolsheretsk	52°50'	156°18'	30	1966–2020
32583	Petropavlovsk-Kamchatsky	52°59'	158°39'	32	1894–2020

Peninsula (Table 2, Figure 1), which have operated almost continuously since the 1960s and some of them started in the 1930s. The oldest station in this region is Petropavlovsk-Kamchatsky, the data here is available since 1894. We used both the data at meteorological times (air temperature, cloud cover, snow depth) and average daily characteristics (air temperature and precipitation (Bulygina

et al., 2014a, b, c)). The percentage of missing values is less than 9% except for Semyachik station, where it is equal to 16%. The monthly averages were calculated if the half of daily values in the month were available and the seasonal averages – when more than 1 month was available. The data were obtained from the Russian climate archive of RIHMI-WDC.

The number of meteorological stations in the Kamchatka Peninsula unfortunately is not sufficient for the investigation of the climatic anomalies spatial structure in detail: most meteorological stations are located on the coast (Figure 1) and far from the selected glacial regions. Therefore, the latest version of ECMWF Reanalysis ERA5 (ERA5: data documentation...) was also used, with hourly and monthly temporal resolution and spatial resolution of 31 km (on the grid  $0.25^\circ \times 0.25^\circ$ ) for the years 1979–2020, the parameters used in this work are presented in Table 3. The time period started only from 1979 to exclude relatively low-quality reanalysis data before the 1970s (less available observational data (Chen et al., 2008)) as well as to include the start of modern global warming (Gruza & Rankova, 2012; IPCC, 2021).

## 4 | METHODOLOGY

### 4.1 | Glaciation area and its changes

The glacier boundaries on modern satellite images were interpreted manually in accordance with the methodology of the International GLIMS project (Raup & Khalsa, 2010). The Landsat-7 image of 9 June 2000 was preliminarily prepared as follows before interpretation: a synthesized image was created from channels B3, B4 and B5 with a spatial resolution of 30 m, which was pan-

sharpened with data from the B8 channel with a spatial resolution of 15 m.

Satellite images used in our work and previous works (Muraviev, 2020a; Muraviev & Nosenko, 2013) were selected at the end of the ablation period before the first snowfalls. This has reduced the influence of seasonal snow cover and snowfields on the results of interpretation of glacier boundaries. The second criterion in the selection of satellite images was the absence of clouds over the glaciers.

The errors in glacier area estimates were determined as follows:

- as a product of the glacier boundaries length and the accuracy of images spatial referencing (about 11 m with a confidence level of 95.5%) (SENTINEL, 2020) for the data from Sentinel-2 images (Muraviev, 2020a).
- as the product of the glacier boundaries length and the resolution of the B8 panchromatic channel (15 m) as a result of processing data from the Landsat-7 image interpretation.
- as a product of the glacier boundaries length and their resolution (15 m) as a result of processing ASTER image interpretation data (Muraviev, 2020a)

The main information about the glaciers of the northern part of the Sredinny Range in the Catalogue of Glaciers of the USSR (Vinogradov, 1968) was obtained from the analysis of aerial photographs of 1950, and the information about the glaciers of the Kronotsky Peninsula was obtained from the processing of aerial photographs of the year 1957, supplemented by fieldwork data in 1960. The Catalogue of Glaciers of the USSR does not contain accurate data on the glaciers boundary's location. The Information about the glacier's location and their shape in the plan is given in a schematic form and is not suitable for measurements. This Catalogue recorded glaciers with an area of more than  $0.1 \text{ km}^2$ .

It is not possible to estimate the area errors for all glaciers in the study areas registered in The Catalogue of Glaciers of the USSR (Vinogradov, 1968), since the original aerial photography data are not available. However, in some cases it was possible. In Muraviev and Nosenko (2013), it was made for the Slyunin and Grechishkin glaciers located in the northern part of the Sredinny Range. From processing the data of these glaciers' boundaries interpretation on registered aerial photographs of 1950, it was shown that the resulting areas differ from the data of the Catalogue of Glaciers of the USSR (Vinogradov, 1968) by 0.7% for the Slyunin glacier and by 2.2% for the Grechishkin glacier. For the area of the Kronotsky Peninsula, the data of the Catalogue of Glaciers of the USSR were

**TABLE 3** Meteorological parameters by ERA5 Reanalysis for the period 1979–2020 are used in this work.

Name	Vertical level	Units
Air temperature	2 m	$^\circ\text{C}$
Precipitation	Surface	$\text{m}\cdot\text{day}^{-1}$
Horizontal components of wind ( $u, v$ )	10 m; 500–1000 hPa (step 50 hPa)	$\text{m}\cdot\text{s}^{-1}$
Analogue of vertical velocity ( $w$ )	500–1000 hPa (step 50 hPa)	$\text{Pa}\cdot\text{s}^{-1}$
Divergence of wind speed	500–1000 hPa (step 50 hPa)	$\text{s}^{-1}$
Atmospheric pressure	Surface	hPa
Geopotential height	500 hPa	m
Downward shortwave radiation, net shortwave radiation	Surface	$\text{W}\cdot\text{m}^{-2}$
Downward longwave radiation, net longwave radiation	Surface	$\text{W}\cdot\text{m}^{-2}$
Cloud cover	Integral	Fraction

checked on the Koryto and Levy Tyushevsky glaciers. When comparing the obtained results with the data of the Catalogue, it was found that the discrepancy in the areas for the Koryto glacier is 3%, and for the Levy Tyushevsky glacier – 3.9% (Muraviev, 2017).

To determine the glaciers altitudinal characteristics the ArcticDEM v3.0 DEM mosaic (Porter et al., 2018) with a spatial resolution of 2 m was used. For the northern part of the Sredinny Range (Muraviev, 2020a) the datasets of 29 August 2018–30 August 2018 were used. The analysis of the glacier area dynamics on the Kronotsky Peninsula in this study was based on the data from 06/23/2020 DEM ASTER GDEM V3 (NASA/METI/AIST/Japan Space Systems & U.S./Japan ASTER Science Team, 2018), which was used similarly to ArcticDEM v3.0 for six glaciers in the northern part of the Sredinny Range that were not covered by ArcticDEM v3.0. For the Kronotsky Peninsula ASTER GDEM V3 was used to cover several small areas not covered by the ArcticDEM v3.0 data.

Also, the ArcticDEM v3.0 mosaic (Porter et al., 2018) was used as extra data for drawing glacial divides. For this purpose, raster images of the exposure and slope of the surface were built, which significantly increase the accuracy of drawing glacial divides, compared with interpretation based on visual features. It should be noted that the conduct of glacial divides in the Catalogue of Glaciers of the USSR (Vinogradov, 1968) and in the present study may differ significantly. Therefore, in some cases, the analysis of changes in individual glacier areas that have extended glacial divides with the other glaciers doesn't make sense. In such cases, changes in the area of the entire group of glaciers with common glacial divides should be analysed.

For the statistical analysis of glaciation changes in the northern part of the Sredinny Range (Muraviev, 2020a) glaciers were divided into groups according to their areas in 2016–2017. In the case of glaciers division into parts, registered in the Catalogue of Glaciers of the USSR (Vinogradov, 1968 or Muraviev & Nosenko, 2013), the total area of all fragments of divided glaciers in 2016–2017 was taken into account. For Kronotsky Peninsula glaciers were divided into groups according to their areas in 2019. In the case of division into fragments 2019 of glaciers registered in the Catalogue of Glaciers of the USSR (Vinogradov, 1968), the total area of all fragments was taken into account.

All satellite images and DEM used in this work were recorded in the UTM projection (zone 57N) on the WGS 1984 ellipsoid. Remote sensing data were processed in the ESRI ArcGIS and QGIS software packages. Statistical processing was carried out in LibreOffice Calc.

## 4.2 | Climate changes

Estimates of climate averages and linear trends were carried out for a single period for all data – 1979–2020, except the stations near selected glaciological areas – their data are presented from the year 1950. The linear trend was calculated using the least squares method, its significance was determined by Student's parametric criteria (Gandin & Kagan, 1976; Isaev, 1988). In Shkaberda (2015) it was shown that most of the annual and monthly series of air temperature and precipitation at meteorological stations in Kamchatka follow a normal statistical distribution, therefore, to assess the significance of trends, it is correctly to use parametric criteria (such as Student's *t*-test).

The calculations were carried out using the Python programming language and the MS Excel package; maps and graphs of climate parameters were built in the Python libraries Matplotlib and Basemap.

### 4.2.1 | Assessment of the grid climate data reliability

Since the data of grid archives contain errors, it is necessary to compare them with the reference source of information, that is, with the data of weather stations. For this purpose, ERA5 data has been interpolated to station points. For both air temperature and precipitation, Pearson's correlation coefficients are significant according to the Student's *t*-test at a significance level of 5%. For air temperature, the correlation coefficient between the station data and the reanalysis turned out to be higher than 0.85 (Figure 2a). Relative deviations of monthly air temperatures on average for the period for all stations do not exceed 50% of the standard deviation absolute value (Figure 2c). The monthly precipitation data by ERA5 reanalysis for the same period also show relatively high correlation coefficients (Figure 2b) – at all stations, it is higher than 0.6. For most points, the relative deviations do not exceed 50% of the standard deviation in absolute value (Figure 2d), and the highest values are observed for stations in the central part of the peninsula: up to 137%. Apparently, this is due to the significant contribution of mesoscale processes in the Kamchatka River valley between the two main ridges of the peninsula: Vostochny and Sredinny, which are poorly reproduced by the global ECSMF model (ERA5 reanalysis).

The nearest weather stations are located at a distance of 100–150 km from the test areas where the analysis of glaciation area trends was performed (Figure 1). Therefore, at least general estimates of the spatial homogeneity of the monthly air temperature and precipitation fields

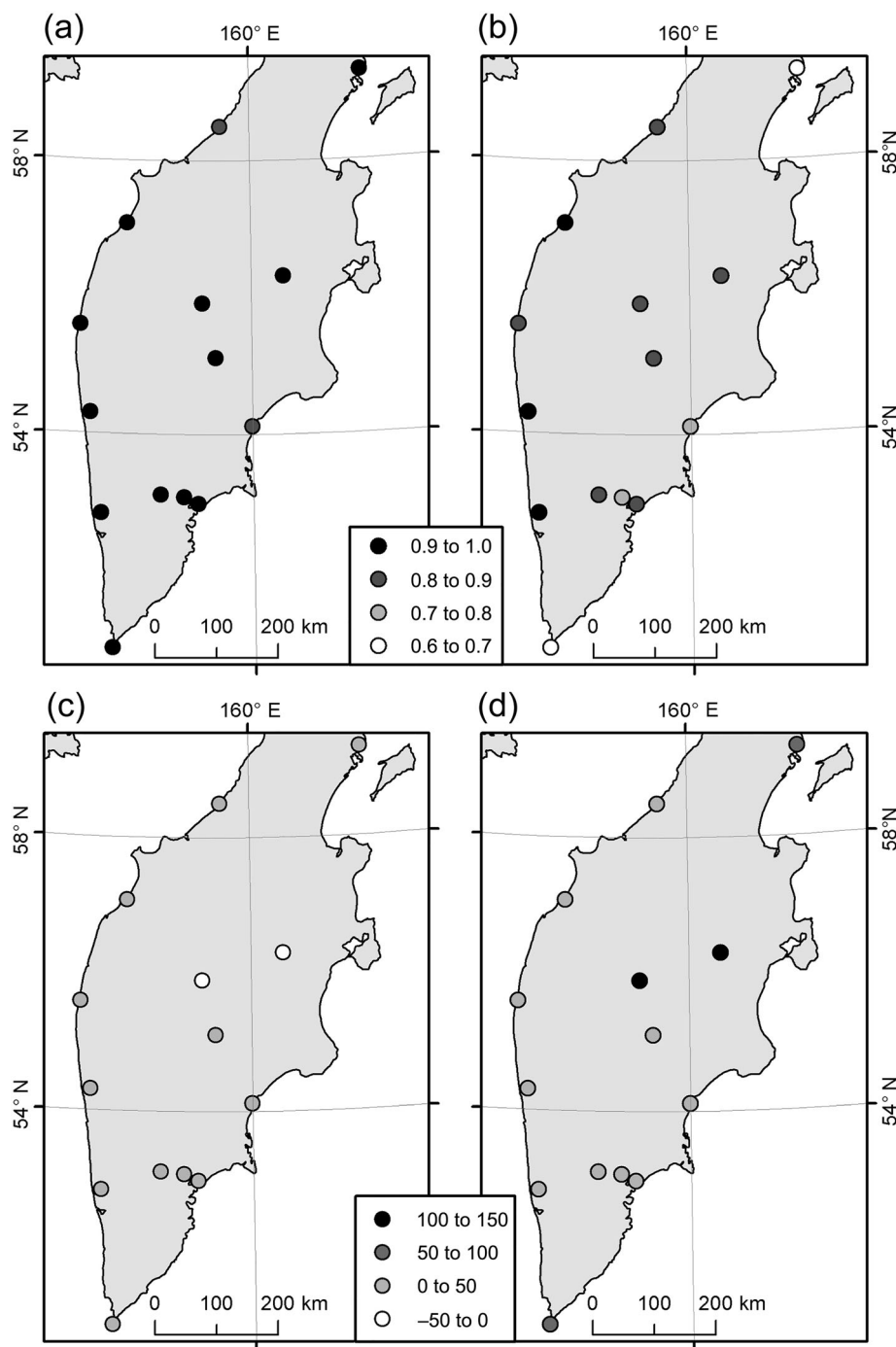


**FIGURE 2** Quality assessment of ERA5 data on the Kamchatka Peninsula for the period 1966–2020: Pearson correlation coefficients at station points for monthly air temperatures time series (a) and monthly precipitation time series (b) according to weather stations and ERA5 reanalysis; average relative deviations (in % of weather station data standard deviation) of monthly mean air temperatures (c) and monthly precipitation sums (d) according to ERA5 reanalysis data.

are required. One of the basic spatial homogeneity measures of the field is a spatial correlation function, which is the dependence of the normalized correlation coefficient on the distance (Gandin & Kagan, 1976). This function was calculated for three meteorological stations located near the areas of glaciation characteristics trend assessment: Ust-Voiampolka, Esso and Semyachik. For mean monthly air temperature, the normalized coefficient of spatial correlation for each weather station is higher than 0.9, which demonstrates a very high spatial homogeneity of this parameter. Based on this, it can be

concluded that the weather stations of the peninsula reliably describe the thermal regime of the areas where glacier dynamics' assessment was made.

The correlation function of total precipitation for the hydrological year (October–September), calculated for the stations of Kamchatka in Glazyrin et al. (1985), showed that the circulation processes over the seas surrounding Kamchatka are the same in time, and the main role in precipitation distribution in the interior of the peninsula plays the relief. The estimation of the spatial correlation function performed in this work confirms the



value of the correlation radius of about 150 km (if the threshold value of the correlation coefficient is 0.6). Based on these considerations, we can conclude that the Esso weather station describes well the precipitation of the southern part of the test area within the Sredinny Range and the entire test area of the Kronotsky Peninsula (Figure 3).

The Ust-Voiampolka weather station is located approximately 99 km from the northernmost glacier of the Sredinny Range; therefore, it can be said that its data characterize the background precipitation falling on the glaciers of the northern part of the Sredinny Range (Figure 1). The Semyachik station is located approximately 130–150 km from the Kronotsky glaciers, that is, they are located within the radius of a significant correlation. As a result, we can conclude that the observation network in Kamchatka describes the precipitation field much worse than the air temperature field. However, most of the studied mountain–glacier regions fall into the area of significant correlation.

#### 4.2.2 | Spatial uncertainties in mountain areas

As it was mentioned above, most of the weather stations in Kamchatka are situated on the coast or in low-land areas (less than 500 m, see Table 2), but the glacier areas considered in our work are situated at altitudes up to 2500 m (as in the case with the northern part of the

Sredinny Range). Thus, we almost don't have any information about the climate in mountain areas except the reanalysis data. Nevertheless, in this work, we don't analyse the absolute values of the climate parameters, but only their tendencies for recent decades. So, we assume that the coefficients of linear trends of the main meteorological parameters almost don't change with the increasing altitudes, or change slightly.

In Toropov et al. (2019), it was obtained that the air temperature trends in Caucasus were decreasing from the 1500 m height by the stations data and reanalysis ERA-Interim data. The tendency for to warming rate to decrease with the altitude was also revealed in other works (Sherwood et al., 2008; Vuille & Bradley, 2000). In the case of the precipitation trend, there were no significant changes in the altitude noted in Caucasus (Toropov et al., 2019).

## 5 | RESULTS

### 5.1 | Glaciation area changes

In 2016–2017, there were 465 glaciers with a total area of  $255 \pm 17 \text{ km}^2$  in the northern part of the Sredinny Range according to the work of Muraviev (2020a). A quantitative comparison with the Catalogue of Glaciers of the USSR (Vinogradov, 1968) showed that 106 glaciers retained their integrity, 46 broke up into 143 fragments and 45 glaciers were not found on modern Sentinel-2 satellite images.

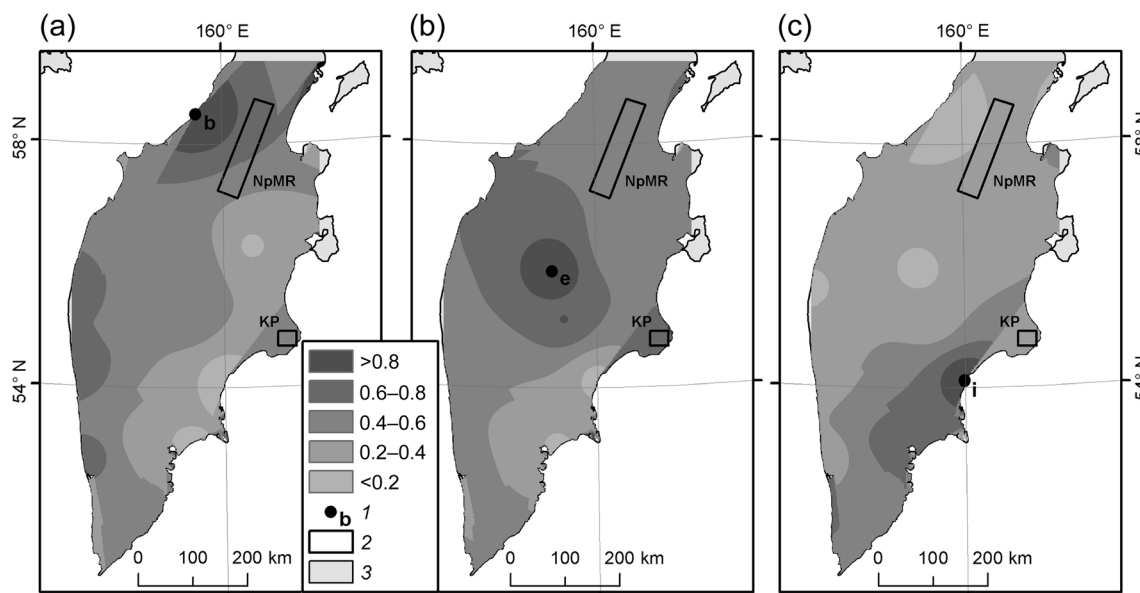


**FIGURE 3** Spatial correlation of monthly precipitation sums for weather stations: Ust-Voiampolka (a), Esso (b), Semyachik (c). 1 – weather station location (Ust-Voiampolka-b, Esso-e и Semyachik-i), 2 – the location of test areas at the northern part of Sredinny Range (NpMR) and the Kronotsky Peninsula (KP), 3 – the areas not covered by spatial correlation function estimates.

In total, 197 glaciers were registered in the Catalogue of Glaciers of the USSR (Vinogradov, 1968) for the territory of the northern part of the Sredinny Range. Obviously, their number was significantly underestimated. The northern part of the Sredinny Range is characterized by a large amount of snow in winters and a wide distribution of large perennial snow patches (Vinogradov & Ogorodov, 1966). Probably, when compiling the Catalogue of Glaciers (Vinogradov, 1968), many small glaciers were mistaken for large perennial snow patches and were not included in it. It should also be taken into account that the Catalogue of Glaciers (Vinogradov, 1968) recorded glaciers with an area of at least 0.1 km<sup>2</sup>. In the work by Muraviev and Nosenko (2013), 190 glaciers were identified in this area that were not registered in the Catalogue of Glaciers of the USSR. In total, 55 of them had an area of less than 0.1 km<sup>2</sup>, and the area of another 116 was in the range of 0.1–0.5 km<sup>2</sup>.

Thus, according to the RGI 6.0 Catalog (RGI Consortium, 2017), there are 533 glaciers with a total area of about 421 km<sup>2</sup> in the northern part of the Sredinny Range. RGI 6.0 data covering the study area were obtained as a result of automatic interpretation of glacier boundaries on satellite images from 2000 to 2011. The glacier inventory in the northern part of the Sredinny Range carried out by Muraviev and Nosenko (2013) showed that in 2002 there were 388 glaciers in this area with a total area of about 335 km<sup>2</sup>. Only 32 glaciers found on modern Sentinel-2 images were not previously recorded in works (Muraviev & Nosenko, 2013; Vinogradov, 1968). Some of them are outside the coverage area of the 2002 ASTER satellite images and schemes of the Catalogue of Glaciers of the USSR.

In this context, the change in the area of glaciers for different time periods was calculated for two different samples. Table 4 presents data on glacier area changes in

the northern part of the Sredinny Range, registered in the Catalogue of Glaciers of the USSR (Vinogradov, 1968) and found on modern Sentinel-2 satellite images (Muraviev, 2020a). A significant part of the glaciers broke up into smaller fragments, so 152 glaciers registered in the Catalogue (Vinogradov, 1968) corresponded to 187 glaciers interpreted in 2002 and 249 – in 2016–2017. From 1950 to 2016–2017 the total area reduction of these glaciers was about 125 km<sup>2</sup> or 35.6%. At the same time, approximately half of the reduction (about 62 km<sup>2</sup>) occurred in the period 1950–2002, which is 1.20 km<sup>2</sup> or 0.34% of the initial glacier area per year. The remaining losses (63 km<sup>2</sup>) occurred in the period from 2002 to 2016–2017, which is 4.20 km<sup>2</sup> or 1.45% of the area per year. This means that the reduction rate of this glacier group in the period from 2002 to 2016–2017 increased by about 4.3 times compared with the period 1950–2002.

The glacier area reduction in the northern part of the Sredinny Range in all three periods turned out to be inversely proportional to their size (see Table 4). The smallest reduction (10.9%) compared to the data from the Catalogue of Glaciers of the USSR (Vinogradov, 1968) was experienced by the largest (>5 km<sup>2</sup>) glaciers (Muraviev, 2020a). The greatest reduction is observed in glaciers with an area of less than 0.1 km<sup>2</sup>. Simultaneously with the glaciers area reduction, they disintegrated into smaller fragments. Thus, 46 glaciers registered in the Catalogue of Glaciers of the USSR (Vinogradov, 1968) disintegrated into 81 fragments by 2002, and by 2016–2017 – into 143 fragments.

An analysis of the glacier area reduction, depending on their exposition according to the Catalogue of Glaciers of the USSR (Vinogradov, 1968), showed that the maximum decline for the period from 1950 to 2016–2017 was observed for the glaciers oriented to the southeast (by 62.9% or 19.6 km<sup>2</sup>) and south (by 43.6% or 5.0 km<sup>2</sup>)

**TABLE 4** The changes in the area of glaciers of different sizes in the northern part of the Sredinny Range, registered in the Catalogue of Glaciers of the USSR (Vinogradov, 1968) and found on modern Sentinel-2 images from 1950 to 2016–2017 (based on work (Muraviev, 2020a, 2020b)).

Glacier size in 2016–2017, km <sup>2</sup>	Glacier area, km <sup>2</sup>			Glacier area changes, km <sup>2</sup> /%		
	1950	2002	2016–2017	1950–2016–2017	1950–2002	2002–201–2017
>5	132.7	134.5 ± 7.7	118.2 ± 4.0	–14.5/–10.9	1.8/1.4	–16.3/–12.1
2–5	65.7	55.6 ± 5.2	43.2 ± 2.7	–22.5/–34.2	–10.1/–15.4	–12.4/–22.3
1–2	59.3	45.1 ± 5.5	32.2 ± 2.6	–27.1/–45.7	–14.2/–23.9	–12.9/–28.6
0.5–1	36.1	22.9 ± 3.0	15.2 ± 1.5	–20.9/–57.9	–13.2/–36.6	–7.7/–33.7
0.1–0.5	49.8	28.0 ± 4.7	16.5 ± 2.2	–33.3/–66.9	–21.8/–43.8	–11.5/–41.1
<0.1	7.9	3.2 ± 0.7	0.9 ± 0.2	–7.0/–88.6	–4.7/–59.5	–2.3/–71.0
Total	351.5	289.3 ± 26.8	226.2 ± 13.2	–125.3/–35.6	–62.2/–17.7	–63.0/–21.8

**TABLE 5** Change in the area of glaciers of different sizes in the northern part of the Sredinny Range, recorded in the work (Muraviev & Nosenko, 2013), from 2002 to 2016–2017 (based on the work (Muraviev, 2020a, 2020b)).

Glacier size in 2016–2017, km <sup>2</sup>	Glacier area, km <sup>2</sup>		Glacier area change from 2002 to 2016–2017, km <sup>2</sup> /%
	2002	2016–2017	
>5	128.4 ± 7.1	112.6 ± 3.7	−15.8/−12.3
2–5	59.1 ± 5.3	46.5 ± 2.7	−12.6/−21.3
1–2	41.4 ± 4.6	30.2 ± 2.2	−11.2/−27.1
0.5–1	33.3 ± 3.9	21.1 ± 1.9	−12.2/−36.6
0.1–0.5	59.8 ± 10.8	35.0 ± 4.9	−24.8/−41.5
<0.1	16.8 ± 4.3	5.3 ± 1.4	−11.5/−68.5
Total	338.8 ± 36.0	250.7 ± 16.8	−88.1/−26.0

(Muraviev, 2020a). These groups of glaciers are also characterized by the largest area reduction in the years 1950–2002 (by 42.1% and 23.0%, respectively) and from 1950 to 2016–2017 (by 35.9% and 26.7%, respectively). It should be noted that glaciers of southeastern and southern expositions, compared to glaciers of other expositions, have relatively small average sizes both according to the Catalogue (Vinogradov, 1968) and according to the data of 2002 and 2016–2017 years.

A minimum decrease in glacier area from 1950 to 2016–2017 occurred for glaciers oriented to the northeast (by 25.8% or 13.5 km<sup>2</sup>), southwest (by 29.4% or 13.1 km<sup>2</sup>) and north (by 29.7% or 11.1 km<sup>2</sup>) (Muraviev, 2020a). For glaciers with northeastern and southwestern expositions, such dynamics can be explained by two reasons. Firstly, this is the orientation of these glaciers to the moisture-carrying air masses coming from the Sea of Okhotsk and the Bering Sea from the west and east, respectively. Secondly, the glaciers of these expositions are characterized by the biggest average sizes in the study area.

For further understanding of the glaciation changes of the northern part of the Sredinny Range in the period from 2002 to 2016–2017 the changes in the areas of 344 glaciers identified on the ASTER images dated 18 August 2002, and the corresponding areas of 433 glaciers identified on the modern Sentinel-2 images (Muraviev, 2020a) were analysed. Table 5 presents data on glacier area changes in the northern part of the Sredinny Range, recorded in Muraviev and Nosenko (2013) and found on modern Sentinel-2 images (Muraviev, 2020a). The glacier area reduction, as for the sample in Table 4, turned out to be inversely proportional to their size. The total reduction in the area of these glaciers was 88.1 km<sup>2</sup> (26.0%). The average reduction rate was 1.73% (5.87 km<sup>2</sup>) of the original area (2002) per year. This is significantly higher than the average reduction rate (1.45%) of the sample of glaciers presented in Table 4. The difference is explained by the fact that the glaciers that are not included in the Catalogue of Glaciers of the USSR, included in the

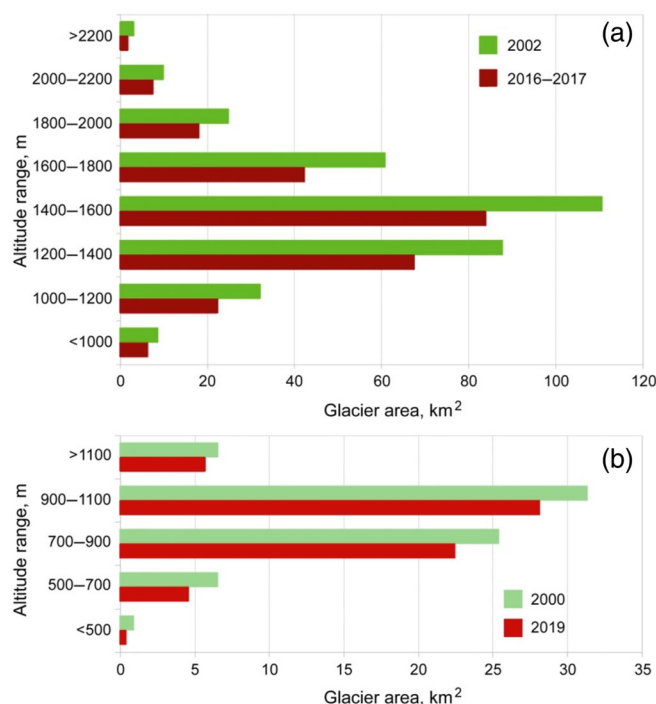


**FIGURE 4** Altitude distribution of glaciation area in the northern part of the Sredinny Range in 2002 and 2016–2017 (a), and in the Kronotsky Peninsula in 2000 and 2019 (b). [Colour figure can be viewed at [wileyonlinelibrary.com](http://wileyonlinelibrary.com)]

sample of Table 5, have a small area (<0.5 km<sup>2</sup>) and are decreasing in size much faster than larger glaciers.

Muraviev (2020a) studied the glaciation decline from 2002 to 2016–2017 by altitude zones (Figure 4a). Most of the glaciation in the northern part of the Sredinny Range (76.6% in 2002 and 77.4% in 2016–2017) is concentrated in the altitudinal range of 1200–1800 m. The main glacier losses from 2002 to 2016–2017 also occurred in this altitude zone – 65.5 km<sup>2</sup> (25.2%) with a total reduction in glaciers for this period by 88.1 km<sup>2</sup>. The percentage of glaciation area below 1000 m from 2002 to 2016–2017 has not changed and is equal to 2.6%.

**TABLE 6** Change in the area of glaciers of different sizes on the Kronotsky Peninsula, registered in the Catalogue of Glaciers of the USSR (Vinogradov, 1968) in 1957–2000–2019.

Glacier size in the year 2019, km <sup>2</sup>	Glacier area, km <sup>2</sup>			Glacier area changes, km <sup>2</sup> /%		
	1957	2000	2019	1957–2019	1957–2000	2000–2019
>5	24.5	24.0 ± 0.9	21.7 ± 0.7	−2.8/−11.4	−0.5/−2.0	−2.3/−9.6
2–5	38.6	28.1 ± 1.6	24.4 ± 1.2	−14.2/−36.8	−10.5/−27.2	−3.7/−13.2
1–2	11.3	7.9 ± 0.7	6.5 ± 0.5	−4.8/−42.5	−3.4/−30.1	−1.4/−17.7
0.5–1	5.4	4.0 ± 0.3	3.1 ± 0.3	−2.3/−42.6	−1.4/−25.9	−0.9/−22.5
0.1–0.5	9.5	2.6 ± 0.4	2.3 ± 0.3	−7.2/−75.8	−6.9/−72.6	−0.3/−11.5
<0.1	0.9	0.1 ± 0.0	0.1 ± 0.0	−0.8/−88.9	−0.8/−88.9	0.0/0.0
Total	90.2	66.7 ± 3.9	58.1 ± 3.0	−32.1/−35.6	−23.5/−26.1	−8.6/−12.9

In 2019, there were 60 glaciers on the Kronotsky Peninsula with a total area of  $61.4 \pm 3.4$  km<sup>2</sup>. A quantitative comparison with the Catalogue of Glaciers of the USSR (Vinogradov, 1968) showed that 26 glaciers retained their integrity, 4 glaciers broke up into 10 fragments, 2 glaciers were not found in the Sentinel-2 image from 09/12/2019. Twenty-four small glaciers with a total area of  $3.3 \pm 0.4$  km<sup>2</sup> are not registered in the Catalogue of Glaciers of the USSR.

Data on the glacier area changes on the Kronotsky Peninsula, registered in the Catalogue of Glaciers of the USSR (Vinogradov, 1968) and found in the Sentinel-2 image dated 12 October 2019, are presented in Table 6. Due to the disintegration of glaciers into smaller fragments, 30 glaciers registered in the Catalogue (Vinogradov, 1968) corresponded to 34 glaciers in 2000 and 35 in 2019. The reduction in the area of these glaciers for 1957–2019 was equal to 32.1 km<sup>2</sup> (35.6%), of which 23.5 km<sup>2</sup> was lost in the period 1957–2000, and another 8.6 km<sup>2</sup> in the period 2000–2019. Thus, the average rate of glaciation area reduction on the Kronotsky Peninsula increased from 0.61% in the years 1957–2000 to 0.67% in 2000–2019.

Glacier area reduction on the Kronotsky Peninsula in the periods 1957–2019 and 1957–2000 was inversely proportional to their size (see Table 5). This pattern was broken for groups of small glaciers (<0.1 and 0.1–0.5 km<sup>2</sup>) in the period 2000–2019. This is probably due to measurement errors in the interpretation of glacier boundaries, caused by the wide distribution of snowfields near the glacier boundaries.

Additionally, the altitudinal distribution of the area of all 60 glaciers of the Kronotsky Peninsula, detected in the Sentinel-2 image on 12 September 2019, in the years 2000 and 2019, was analysed (Figure 4b). More than 82% of the total glaciation area of the region in 2019 was located in the altitudinal range of 700–1100 m, in the year 2000 – more than 80%. The largest glaciation area reduction for

2000–2019 occurred at altitudes below 500 m (55.1%) and 500–700 m (27.9%). The percentage of glaciation located above 1100 m is stable – 9.3% in the years 2000 and 2019.

## 5.2 | Climatic parameters changes

### 5.2.1 | Air temperature

As in most of the globe, the air temperature at all stations on the Kamchatka Peninsula increases in all seasons (Table 7). The warming rate for the period 1966–2020 is higher at stations on the western coast (0.4–0.7°C/10 years) than on the eastern coast of the peninsula (0.3°C/10 years). According to Ippolitov et al. (2008), the average warming rate over the Asian territory of Russia for the period 1975–2005 was 0.34°C/10 years. In Kamchatka, the warming rate is regionally and seasonally dependent: minimum rates are observed in summer and winter (Table 7), and in winter at half of the stations the trend is not statistically significant. If we consider temperature changes in certain months of the year, then the highest warming rate is observed in March: the maximum values are +0.84°C/10 years and 0.9°C/10 years at the stations of the western coast Bolsheretsk and Sobolevo.

Our estimates coincide with those obtained in Shkaberda (2015): the maximum rate of air temperature growth was also found here in March (0.57°C/10 years), the lowest rate was in January and December (0.07–0.08°C/10 years). Cooling in Kamchatka in all winter months, as well as a maximum of warming in March, were revealed in the work of Ippolitov et al. (2008). It is also noted in Shkaberda (2015) and Shkaberda and Vasilevskaya (2014) that on the western coast, the rate of increase in air temperature is higher than on the eastern one: +0.3°C/10 years and +0.14°C/10 years, respectively, for the period 1951–2009. The author



**TABLE 7** Coefficients of the air temperature linear trend (°C/10 years) according to weather stations' data for the period 1966–2020.

Station WMO ID	Station name	Year	Winter	Spring	Summer	Autumn
32213	Mys Lopatka	<b>0.3</b>	<b>0.4</b>	<b>0.3</b>	<b>0.3</b>	<b>0.3</b>
32246	Ossora	0.3	0.1	<b>0.5</b>	<b>0.3</b>	<b>0.5</b>
32252	Ust-Voiampolka	0.2	0.3	<b>0.6</b>	<b>0.2</b>	0.2
32287	Ust-Khayryuzovo	<b>0.4</b>	<b>0.5</b>	<b>0.5</b>	<b>0.3</b>	<b>0.4</b>
32363	Esso	<b>0.5</b>	<b>0.6</b>	<b>0.5</b>	<b>0.4</b>	<b>0.5</b>
32389	Kluchi	<b>0.4</b>	0.3	<b>0.5</b>	<b>0.4</b>	<b>0.5</b>
32411	Icha	<b>0.7</b>	0.3	<b>0.4</b>	<b>0.3</b>	<b>0.4</b>
32447	Dolinovka	<b>0.4</b>	0.4	<b>0.4</b>	<b>0.3</b>	<b>0.4</b>
32477	Sobolevo	<b>0.5</b>	<b>0.7</b>	<b>0.6</b>	<b>0.3</b>	<b>0.4</b>
32509	Semyachik	0.3	0.2	<b>0.3</b>	<b>0.3</b>	<b>0.4</b>
32539	Nachiki	<b>0.5</b>	<b>0.6</b>	<b>0.5</b>	<b>0.4</b>	<b>0.5</b>
32547	Sosnovka	<b>0.3</b>	0.2	<b>0.4</b>	<b>0.3</b>	<b>0.4</b>
32562	Bolsheretsk	<b>0.5</b>	<b>0.6</b>	<b>0.5</b>	<b>0.3</b>	<b>0.5</b>
32583	Petropavlovsk-Kamchatsky	<b>0.3</b>	<b>0.3</b>	<b>0.3</b>	<b>0.3</b>	<b>0.3</b>
Stations' average		0.4	0.4	0.4	0.3	0.4

Note: Values significant at the 5% significance level according to Student's *t*-test are marked in bold.

shows that the period 1971–1980 was relatively cold in all regions of the peninsula, and steady warming began only in 1987.

ERA5 reanalysis data also show a statistically insignificant warming trend in winter, and even a slight cooling in the northern part of the peninsula (Figure 5).

Along with the increase in air temperature, the duration of the frost-free season also increases – with the exception of some stations located on the coasts (Figure 6). At most stations the increase in the duration of the frost-free period is statistically significant and averages 3.5 days/10 years (Figure 6). The number of days with a stable positive temperature is directly related to the duration of the glaciers' ablation period (Ohmura, 2001).

## 5.2.2 | Precipitation

Most weather stations on the Kamchatka Peninsula revealed insignificant trends in precipitation for the period 1966–2020, but there are some stations which showed significant precipitation decreases (Table 8). For example, winter precipitation decline at Mys Lopatka station was equal to  $-22.4\%/10$  years and at Ust-Voiampolka station  $-10\%/10$  years. Significant winter precipitation decrease was also noted at Ust-Khayryuzovo, Dolinovka and Petropavlovsk-Kamchatsky. At Icha station the precipitation has decreased for all seasons. A similar trend of decreasing precipitation at Icha station was found in 1996–2005 at

work (Shatilina & Anzhina, 2008). Ippolitov et al. (2008) showed a decrease in average annual precipitation over the entire territory of Kamchatka to  $-60$  mm/10 years for 1975–2005.

According to the ERA5 reanalysis, precipitation decrease for the years 1950–2020 up to  $-10\%/10$  years was also observed in winter in the northern and central part of the peninsula (Figure 7a), in autumn, and in summer almost for the whole region (Figure 7c). In spring, the precipitation increased. Almost all changes are statistically insignificant according to the Student's *t*-test (except for summer decrease in some areas).

## 5.2.3 | Snow cover

Following the warming in the region, the number of days with stable snow cover has been decreasing during the period of 1966–2020 at almost all stations of the Kamchatka peninsula (Figure 8a,c), most significantly – at coastal stations. The height of snow cover (Figure 8b) has different tendencies – a slight decrease in the inland areas of the peninsula and an increase in some coastal stations, and many of them are statistically insignificant according to Student's *t*-test. An increase in the maximum height of snow cover over the winter, as well as in the number of days with a snow coverage of the station surroundings of more than 50%, was revealed in the central and southern parts of Kamchatka for 1976–2021 in (A Report on climate features, 2022). At stations that are

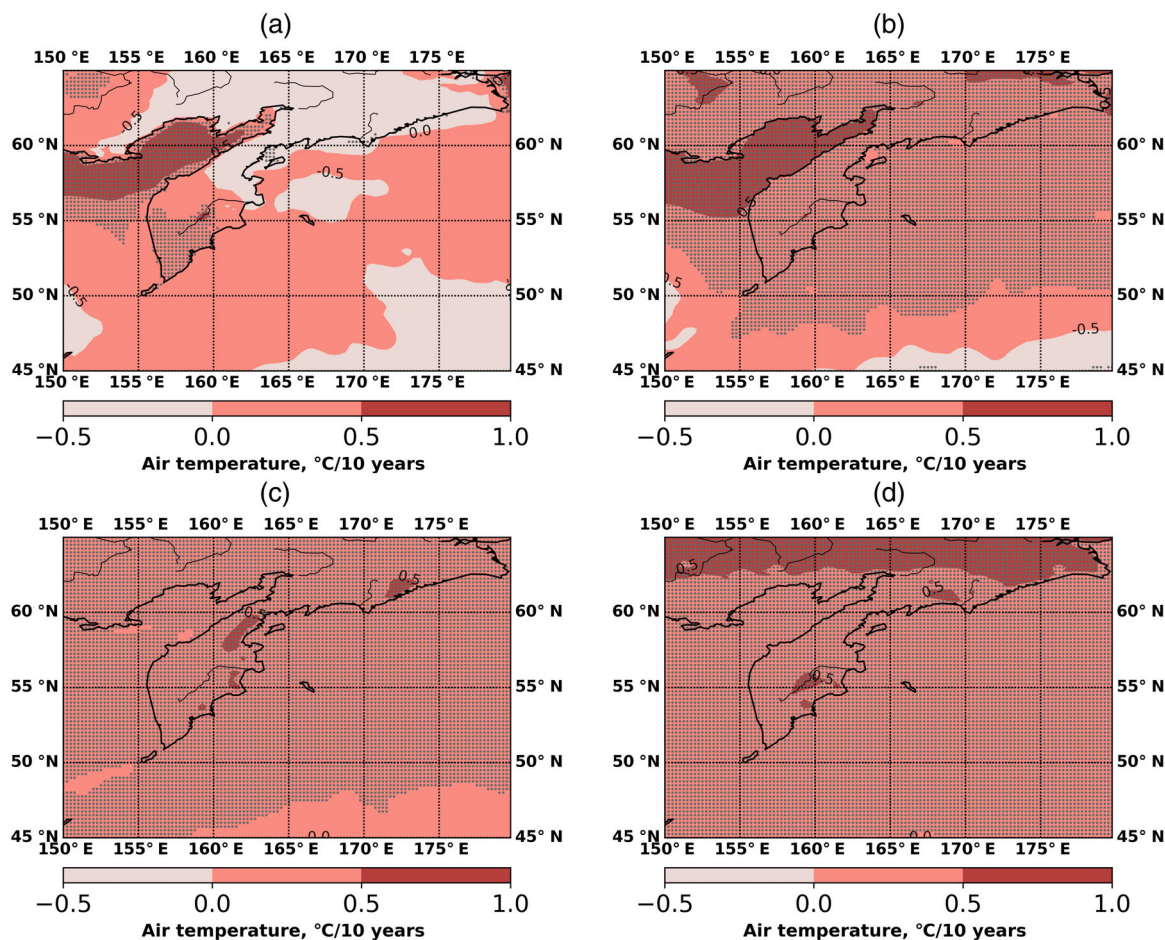


**FIGURE 5** Coefficient of the linear trend of the mean seasonal air temperature for the period 1950–2020 according to the ERA5 reanalysis: (a) winter, (b) spring, (c) summer, (d) autumn. Black shading shows grid points with significant trends at the 5% significance level. [Colour figure can be viewed at [wileyonlinelibrary.com](http://wileyonlinelibrary.com)]

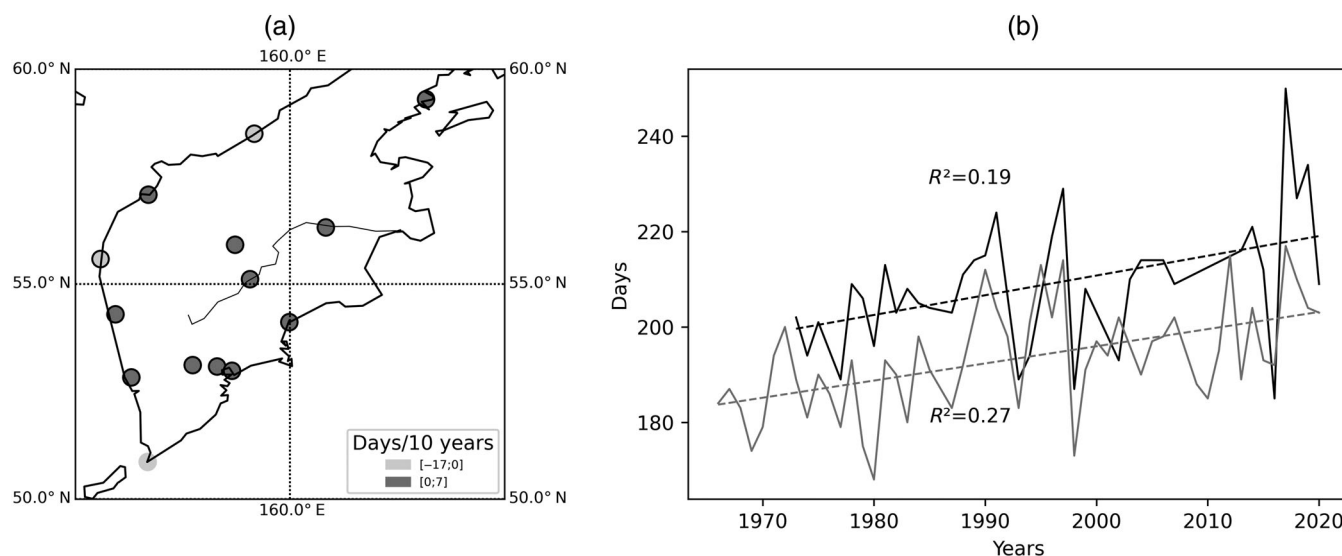


**FIGURE 6** Coefficients of the linear trend (a, days/10 years) of the duration of the frost-free season at the stations of the Kamchatka Peninsula and the time course of the duration of the frost-free season (b) at weather stations Semyachik (black) and Kluchi (grey) for the years 1966–2020. The black circles outline show the points with significant trends at the 5% significance level.

**TABLE 8** Coefficients of precipitation linear trend (%/10 years) according to weather stations for the period 1966–2020.

Station WMO ID	Station name	Year	Winter (DJF)	Spring (MAM)	Summer (JJA)	Autumn (SON)
32213	Mys Lopatka	<b>−8.8</b>	<b>−22.4</b>	−7.9	2.9	<b>−6.0</b>
32246	Ossora	−2.4	−4.0	3.6	−4.0	−2.0
32252	Ust-Voiampolka	<b>−10.3</b>	<b>−10.0</b>	<b>−10.3</b>	−4.0	−1.8
32287	Ust-Khayryuzovo	−3.1	<b>−8.3</b>	−4.7	−4.0	−0.6
32363	Esso	−3.1	−7.1	1.9	−3.8	−2.0
32389	Kluchi	0.8	1.1	4.8	−2.5	1.2
32411	Icha	<b>−14.2</b>	−11.5	<b>−11.3</b>	<b>−12.7</b>	<b>−7.0</b>
32447	Dolinovka	−0.8	<b>−7.5</b>	3.4	−1.7	3.1
32477	Sobolevo	−0.3	1.4	0.1	−4.5	1.3
32509	Semyachik	−3.7	1.3	5.2	−0.5	<b>−9.6</b>
32539	Nachiki	−1.7	−5.7	−0.4	1.6	−1.2
32547	Sosnovka	0.9	−3.3	5.1	−0.8	1.7
32562	Bolsheretsk	0.2	1.5	0.4	−0.1	−1.2
32583	Petropavlovsk-Kamchatsky	<b>−4.0</b>	<b>−9.4</b>	−1.8	−1.4	−1.6

Note: Values significant at the 5% significance level according to Student's *t*-test are marked in bold.

close to the mountain–glacier regions considered in our work (Ust-Voiampolka and Semyachik), a decrease in both characteristics is observed (Figure 8), and for the duration of snow cover it is statistically significant.

#### 5.2.4 | Radiation balance and cloud cover

Air temperature increases during the warm period can be associated with an increase in downward shortwave radiation, which in turn can be caused by an increase in the frequency of fair weather and anticyclonic conditions. In several mountain–glacier regions exactly these processes lead to a mountain glaciation reduction, for example, in the Caucasus (Toropov et al., 2019). According to the ERA5 reanalysis, in Kamchatka, there is an increase in downward shortwave radiation in the warm season (with a maximum in June) which was more pronounced for the last two decades (Figure 9b), up to 15 W/m<sup>2</sup>/10 years in some areas. ERA5 reanalysis data also show a decrease in cloudiness for the years 2003–2020 (within 2%/10 years), however, for station data this trend is observed only at some coastal stations (up to 3%/10 years, Figure 10). Chernokulsky et al. (2011) showed that the total cloudiness and the number of cloudy days according to station data in Kamchatka almost didn't change in summer in 2001–2010 compared to the years 1991–2000, but a significant decrease in cumulus clouds amount occurred at almost all stations in the region in summer and autumn. According

to our estimates (Figure 10d), the lower cloud cover at some stations in Kamchatka and by ERA5 reanalysis data decreased by 2–3%/10 years, and part of the changes are statistically significant at the 5% significance level. The changes in downward solar radiation mostly occur due to lower cloudiness changes, so the shortwave radiation balance increase for the period 2003–2020 can be associated exactly with this process. It should be noted that cloudiness is a rather difficult parameter for analysis, because it has a large spatial variability and depends on local factors, especially in mountain regions, and station data describe cloud conditions in their vicinity (as in the case of precipitation).

For the period of 1950–2002, the most pronounced tendency in radiation characteristics is a decrease in shortwave radiation reflected from the surface (Figure 9c). This effect is observed in May and June and is caused by surface albedo decrease due to an earlier melting of snow cover and sea ice.

The longwave balance for the warm season in most of the Kamchatka Peninsula has a negative trend (Figure 9g,h), which is more pronounced in the years 2003–2020. It is most likely caused by a thermal radiation increase due to surface temperature growth. Another possible factor is a decrease in cloudiness, which may increase the transmission of longwave radiation by the atmosphere. Probably, here these effects turn out to be stronger than the increase in the thermal radiation of the atmosphere due to an increase in its heat and moisture content.



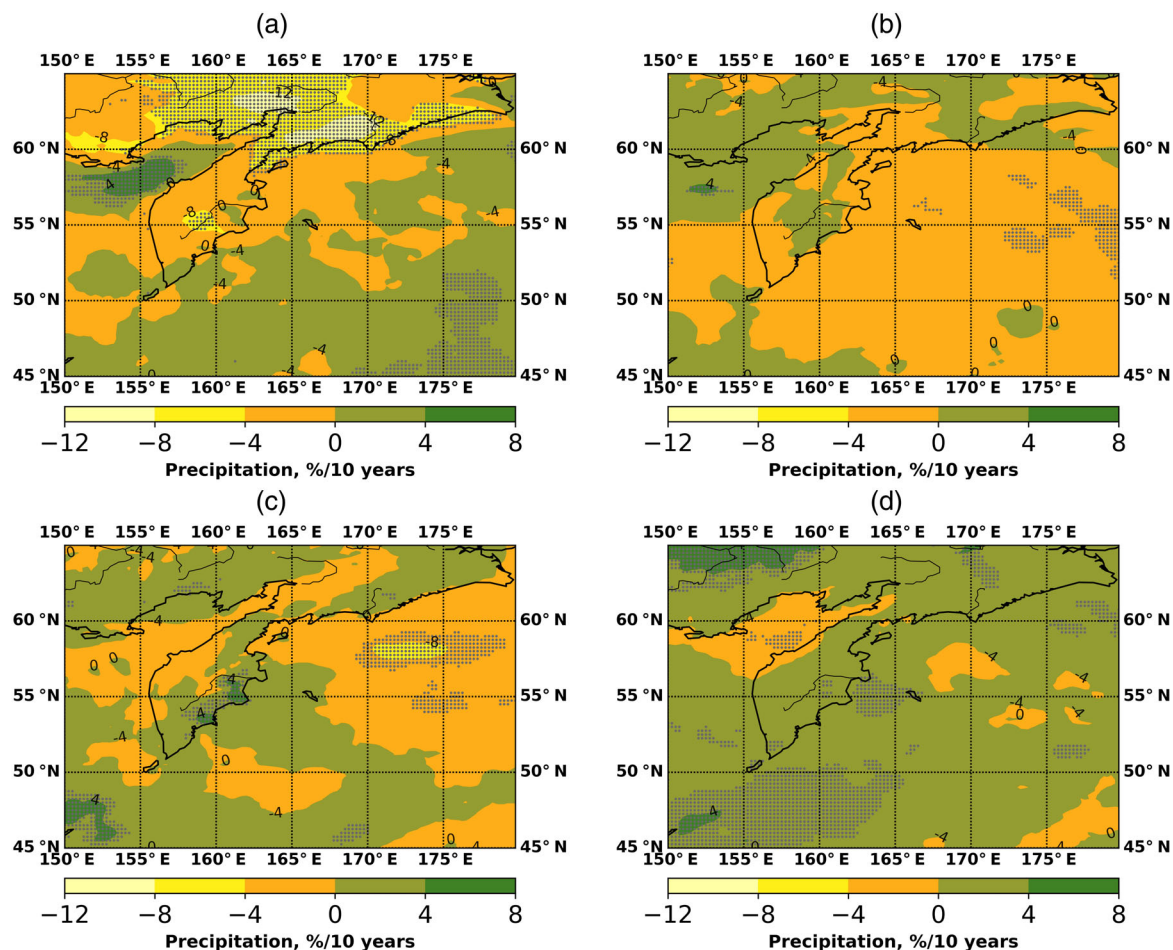


**FIGURE 7** Coefficient of linear trend of seasonal precipitation (a – winter, b – spring, c – summer, d – autumn, %/10 years) for the period 1950–2020 according to ERA5 reanalysis. Black shading shows grid boxes with the significant trend at the 5% significance level. [Colour figure can be viewed at [wileyonlinelibrary.com](http://wileyonlinelibrary.com)]

Thus, the total radiation balance increase in the Kamchatka region for the period of 1950–2002 was connected with the upward shortwave radiation decrease and for the period 2003–2020 – with the downward shortwave increase due to cloud cover decrease.

## 6 | DISCUSSION

### 6.1 | Possible causes of Kamchatka glacier recession

To analyse the climatic factors in glaciation reduction on the Sredinny Range and the Kronotsky Peninsula, the nearest weather stations, Ust-Voiampolka and Semyachik, were chosen. The distance from the weather station to the main glaciers is less than the spatial correlation radius, which was set above. If we follow the classical ‘T-index’ or ‘degree-day factor’ approaches (Ohmura, 2001), we can assume that the glacier dynamics are mainly

influenced by air temperature during the ablation season (on average for the peninsula it coincides with summer period – June–August). According to our results the summer air temperature at both stations slightly (but statistically significant according to the Student test) increased with the same rate – on average about  $0.2^{\circ}\text{C}/10$  years from the year 1950 (Figure 11). Similar values of the air temperature trend were also obtained from the ERA5 reanalysis data (Figure 5c). Such insignificant summer warming could hardly be the reason for the Kamchatka glaciers’ reduction (for example in the Caucasus the summer warming rate is equal to  $0.6\text{--}1^{\circ}\text{C}/10$  years).

Another reason for the intense melting of glaciers may be a precipitation decrease during the accumulation season. Indeed, both according to Ust-Voiampolka weather station data and the ERA5 reanalysis, there was a significant decrease in winter precipitation in the northern part of Kamchatka – up to  $10\%/10$  years (Table 7, Figure 7). Nevertheless, at Semiachik weather station, which is close to the Kronotsky Peninsula precipitation during the



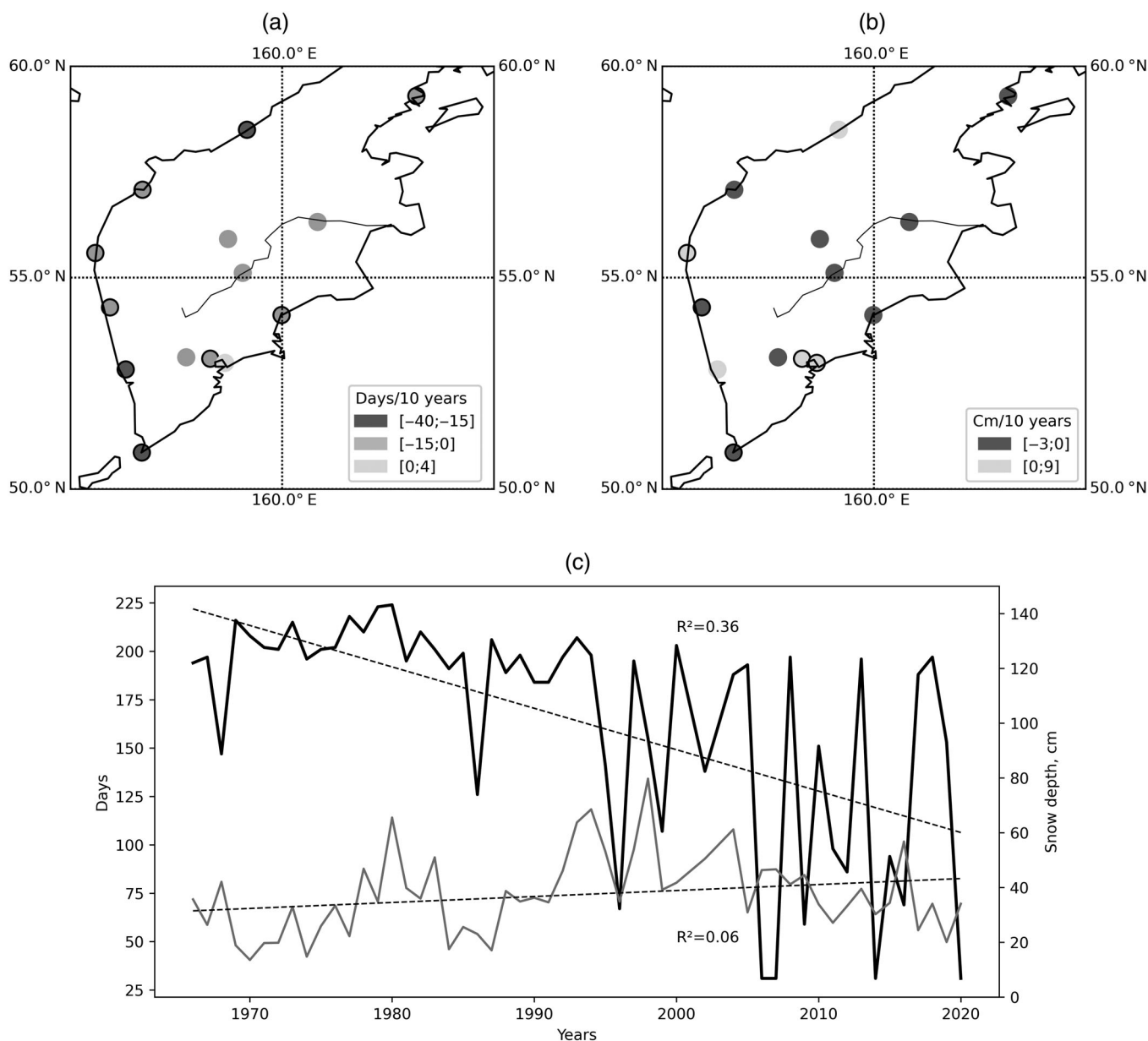


**FIGURE 8** Linear trend coefficients for the number of days with snow cover per year (a) and annual average snow depth (cm/10 years) (b) based on station data for the period 1966–2020; time series of the number of days with snow cover (black line) and snow depth (grey line) for Ust-Voiampolka station (c) for the period 1966–2020. The black circles outline shows the points with significant trends at the 5% significance level.

accumulation season (Figure 11b) and during winter (Table 7) almost haven't changed or slightly (insignificantly) increased.

One more factor that could significantly affect the reduction of glaciation in Kamchatka is a radiation balance, as well as an increase in turbulent heat exchange between the atmosphere and the glacier surface during short but very intense heat advections in the warm season. Increase in the shortwave balance in May–August in 2011–2020 up to  $5 \text{ W} \cdot \text{m}^{-2}$  compared to the beginning of the 21st century, which is observed by ERA5

reanalysis data (Figure 9) is equivalent to a monthly amount of  $41 \text{ MJ} \cdot \text{m}^{-2}$ , which transforms into the melting of an additional 120 mm w.e. of ice, or ablation layer increase by about 25%. In the case of intense warm air advection along the western periphery of an anticyclone located over the Pacific Ocean, cloudy weather is accompanied by a positive temperature anomaly with a strong wind, which leads to a sharp increase in turbulent heat exchange between the ice surface and the atmosphere, and an additional increase in the melting layer.

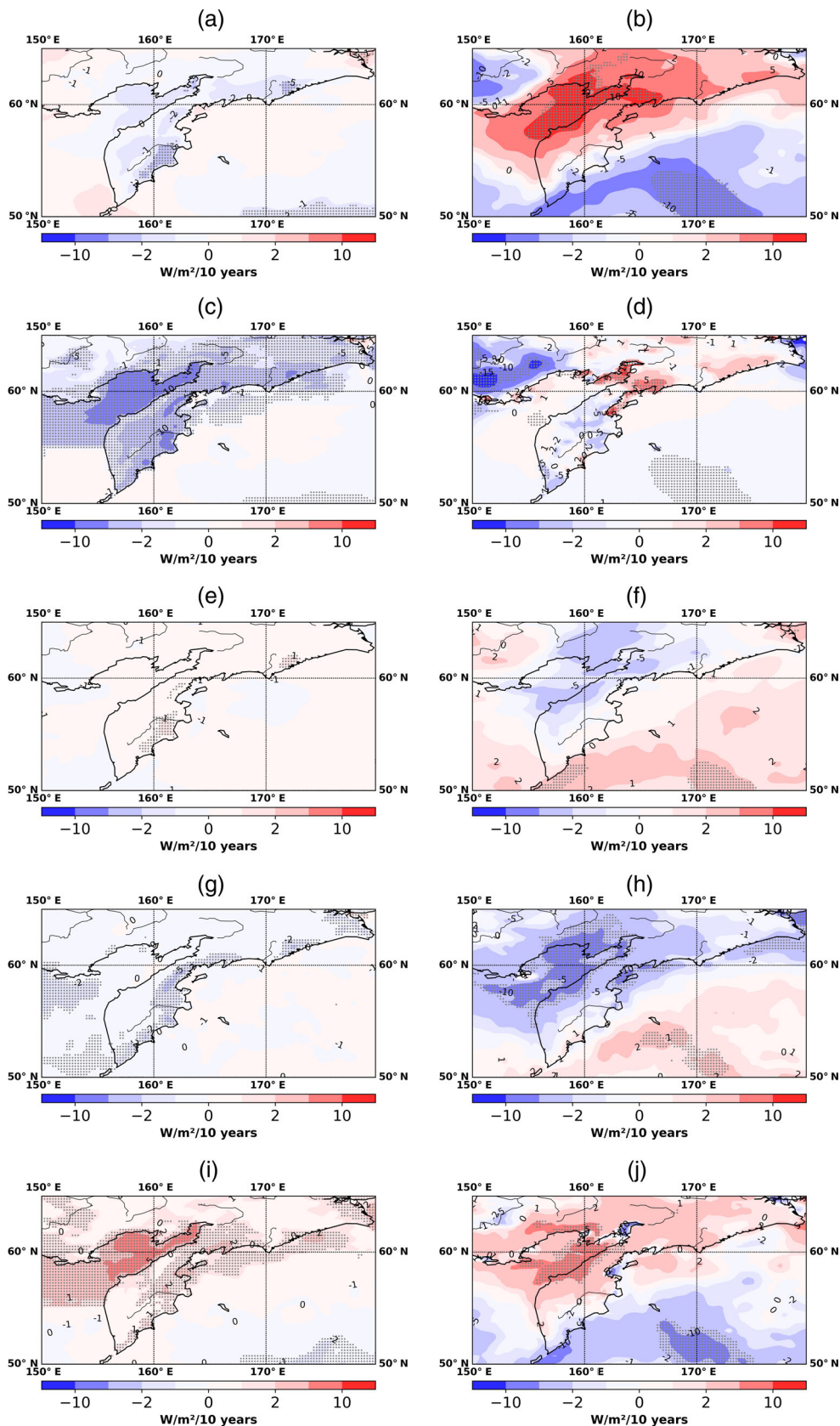


**FIGURE 9** Coefficients of the linear trend in average for May–September of downward shortwave radiation (a, b), upward shortwave radiation (c, d), downward longwave radiation (e, f), net longwave radiation (g, h) and total net radiation balance (i, j) in average for the period 1950–2002 (a, c, e, g, i) and 2003–2020 (b, d, f, h, j) according to ERA5 reanalysis. [Colour figure can be viewed at [wileyonlinelibrary.com](https://onlinelibrary.wiley.com)]

If we assume that the main reason for the degradation of mountain glaciers of the Sredinny Range was an increase in the radiation balance in summer by  $5 \text{ W} \cdot \text{m}^{-2}$  (which is equivalent to an increase in the melting layer by approximately 60 mm/10 years), as well as a decrease in precipitation during the accumulation period by

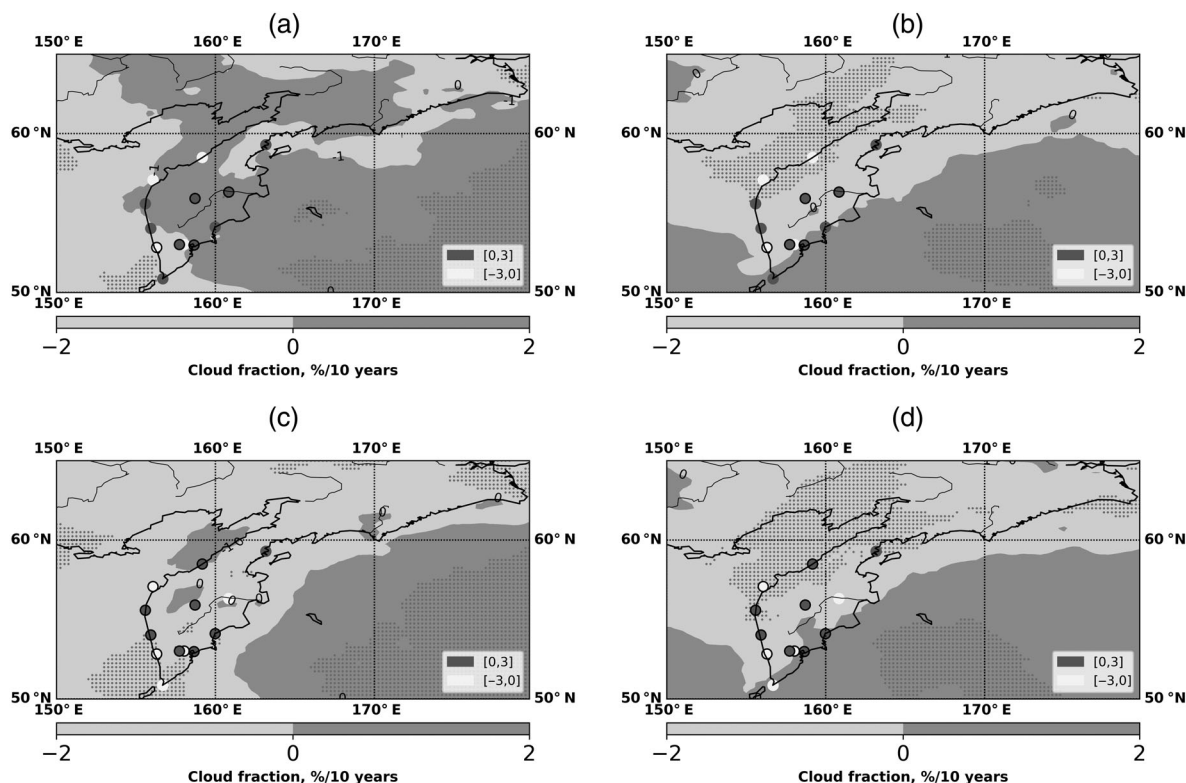


**FIGURE 10** Coefficients of the linear trend of total cloud amount (a, b) and low cloud amount (c, d) in average for May–September for the period 1950–2002 (a, c) and 2003–2020 (b, d) by ERA5 reanalysis data (shading) and weather station data (circles).

approximately the same amount, then we obtain that the average mass balance decrease for the glaciers of the Sredinny Range will be equal to 240 mm for the period 2000–2020 years. Therefore, we can set the annual mass balance trend value to  $-12 \text{ mm} \cdot \text{year}^{-1}$ , and implement a simple numerical experiment for the ‘hypothetical’ glacier of the Sredinny Range with typical morphometric parameters: area –  $3.5 \text{ km}^2$ , length –  $3.5 \text{ km}$ , average thickness –  $30 \text{ m}$ , front width –  $350 \text{ m}$ . The minimal Oerlemans model was used (Oerlemans, 2008), which has proven itself quite well as a tool for describing the modern evolution of typical Caucasus glaciers with detailed meteorological parameters (Toropov et al., 2023). If we start to decrease the mass balance from a value of  $-300 \text{ mm}$  (a typical value for glaciers in Northern Eurasia in the last decade of the XX century), we obtain that for the period 2000–2020, the glacier area in Sredinny Range has decreased by approximately 22%, which is consistent with the observational data given in Table 5. For a typical glacier of the Kronotsky Peninsula, the area reduction has been 11% compared to 13% given in Table 6. Thus, the proposed mechanism of glaciation degradation can be considered a working hypothesis.

According to the data in Tables 1 and 3, the glaciers of the northern part of the Sredinny Range had

experienced the strongest decline in the last 2 decades of the 21st century, while the glaciers of the Kronotsky group, on the contrary, lost a large area in the 20th century. As we can see there are almost no differences in dynamics of air temperatures according to the data of the nearest weather stations (Figure 11). The precipitation revealed slight differences during the last two decades: a decrease at Ust-Voiampolka station and an increase at Semyachik station. The different dynamics of the precipitation in the XXI century on the western and eastern coast of the Kamchatka Peninsula are connected with the changes in large-scale atmospheric circulation over the Asian continent and the northern part of the Pacific Ocean, which are mainly characterized by the indices Pacific Decadal Oscillation (PDO), Pacific-North American Index (PNA) and West Pacific Index (WP). Some studies show that the negative phase of PDO, which prevailed at the beginning of the 21st century, contributed to a weakening of the contrast between temperatures in the tropics and polar regions, and, accordingly, to a weakening of the western transport and an increase in the frequency of blocking anticyclones, in particular, in the Kamchatka region (Bokuchava & Semenov, 2021). The authors (Khen et al., 2019b) wrote that while the PDO index went into the negative phase in 2007, there was a

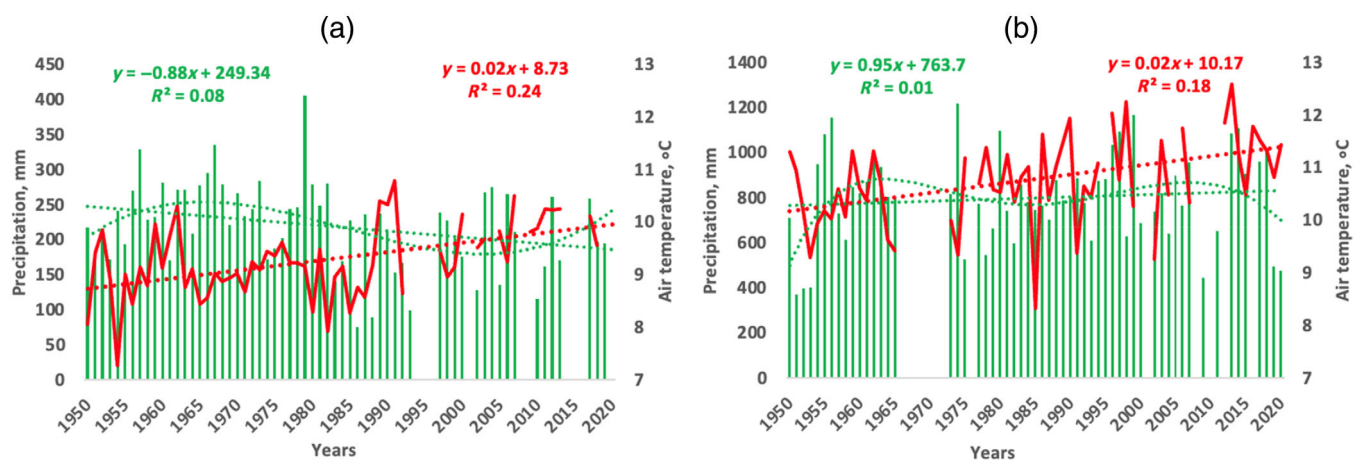


FIGURE 11 Air temperature time series (line) for the ablation season (June–August) and precipitation (histogram) for the accumulation season (October–May) for the years 1950–2020 at stations closest to the glacial region of the Sredinny Range (Ust-Voiampolka (a)) and the glaciation of the Kronotsky Peninsula (Semyachik (b)). [Colour figure can be viewed at [wileyonlinelibrary.com](http://wileyonlinelibrary.com)]

sharp cooling in the Bering Sea and the North Pacific Ocean and positive anomalies in Kamchatka surface temperatures. In the first decade of the 2000s, negative values of the PNA index prevailed. The cold phase of the PNA index is characterized by the predominance of high pressure in the North Pacific Ocean and the weakening of the Aleutian Low (Khen et al., 2019a). The Western Pacific Index WP characterizes the western part of the Pacific Ocean and has the greatest impact on the climate of the Russian Far East and, in particular, the Kamchatka Peninsula (Khen et al., 2019a). The positive phase of the WP index is accompanied by an atmospheric pressure increase over Shelikhov Gulf and weakening of the Aleutian Low, the trajectory of cyclones in the Far East region shifts northward, and air temperature and precipitation increase in Kamchatka and Chukotka (Khen et al., 2019a; Kiktev et al., 2015). In the negative phase, the trajectories of cyclones, on the contrary, shift to the south and there is a shortage of precipitation. Since the 2000s, there was a gradual decrease towards negative values of the Western Pacific WP index. Shatilina and Anzhina (2008) showed that, starting from 1996, the cyclonic depression over the Sea of Okhotsk shifted to the south in the winter season and weakened, which resulted in a precipitation decrease on Kamchatka western coast.

We calculated the correlation coefficients of the average monthly air temperature and precipitation by station data with PDO, PNA, and WP indices for the years 1979–2020: for three stations on the western coast of Kamchatka (Icha, Ust-Khayryuzovo and Ust-Voiampolka), and three stations on the eastern coast (Ossora, Semyachik and Petropavlovsk-Kamchatsky). We found a significant correlation only for precipitation with the WP index:

the coefficients are positive at stations on the western coast and in some months of the cold period reach significant values equal to 0.6, and negative on the eastern coast – from  $-0.3$  to  $-0.6$ . Therefore, the increase in precipitation in the cold season on the eastern Kamchatka coast and the decrease on the western Kamchatka coast can be an additional factor for different glaciers dynamics in selected regions.

The most likely reason for the different dynamics of glaciation in the northern part of the Sredinny Ridge and the Kronotsky Peninsula is the significant differences in their geographical conditions. The glaciation of the Kronotsky Peninsula is located at relatively low altitudes (see Figure 4b). The absolute heights of the low-mountain Kronotsky Range do not exceed 1300 m. It is represented by warm glaciers, the areas of accumulation which are formed by the warm firn ice-formation zone. The glaciers of this region exist due to a large amount of solid precipitation, as a result, the value of accumulation-ablation at the height of the glacier feeding boundary can exceed 4000 mm w.e. (Muravyev et al., 1999; Kotlyakov & Kravtsova, 1997). The glaciers of the northern part of the Sredinny Range are located at much higher altitudes (see Figure 4a). They are of the cold type. Their areas of accumulation are formed by cold firn, firn-ice and ice-formation zones, and the values of accumulation-ablation at the glacier feeding boundary are at least 2 times lower than on the Kronotsky Peninsula (see map no. 234 in Kotlyakov & Kravtsova, 1997).

Note that the study of the dynamics of glaciation in these areas is significantly limited by the availability of materials on the morphometric characteristics of glaciers. Materials of the Catalogue of Glaciers of the USSR (Vinogradov, 1968) are dated 1950 for the



northern part of the Sredinny Ridge and 1957 for the Kronotsky Peninsula. The following time slices, provided with materials of suitable quality, date back to 2002 and 2000 respectively. It is obvious that changes in the glaciers of the study areas during the long periods of 1950–2002 and 1957–2000 could not be uniform, as the climatic conditions were changing. However, there is no additional data on the characteristics of glaciers within these periods.

## 6.2 | Large-scale atmospheric circulation anomalies that caused the Kamchatka glacier recession

To explore the connection between air temperature and radiation anomalies with circulation features, we analysed the trends in 500 hPa geopotential height, vertical velocity and divergence of velocity. It can be seen that there is a significant increase in the geopotential height of the level of 500 mb up to 10 m/10 years in Kamchatka in the warm season, observed from the 1980s (Figure 12a). Mainly positive tendencies in vertical velocity and the increase in velocity divergence are also observed in the Kamchatka region (Figure 12b,c), which indicates an increase in downward air movements. These features confirm the fact that the anticyclonic circulation intensifies for the last decades in the warm season.

We found that the 850 and 500 mb heights growth for the last decades (2000–2020) is associated with the extending of the North Pacific Anticyclone to the North and the forming an additional ridge over the Kamchatka peninsula which enhances the warm advection from the tropics. An increase in the intensity of the North Pacific High at 500 hPa height in July was revealed for the years 1977–2006 in the work (Shatilina & Anzhina, 2008), and the increase in surface pressure in July for 1975–2005 up to 1 hPa/10 years was identified in the work (Ippolitov et al., 2008). Kim et al. (2021) found the North Pacific High extension at 850 hPa height from 1984 to 2018 years.

The North Pacific High extension to the north is probably a part of the process called «expansion of the tropics», when the Hadley Cell expand to the North (Lu et al., 2007). For example, in the recent work of Staten et al. (2018), it was shown that the tropics have widened at the rate of 0.5° latitude per decade since 1979. Correspondingly, the zone of subtropical anticyclones should shift to the north (Seager et al., 2007).

It should be noted that over the continental part of Eastern Asia, a low-pressure system usually forms in the warm season. In Shatilina and Anzhina (2008), it was noted that the weakening of the Asian depression

intensity in summer also contributes to an increase in air temperature on the Asian coast of Russia and the western coast of Kamchatka and an increase in sea surface temperature due to advection of warm continental air masses to the coast. We can see that in the last two decades simultaneously with the atmospheric pressure growth over the Kamchatka region and the Sea of Okhotsk, the growth of geopotential height over the Asian Low has also occurred. These processes probably generated an increase in warm advection and a shortwave radiation balance, which caused the enhanced glacier ablation in the Kamchatka region.

## 7 | CONCLUSION

The glaciation of the northern part of the Sredinny Range and the Kronotsky Peninsula was decreasing from the middle of the XX century to the beginning of the XXI century. Simultaneously with the glacier area reduction in both regions, their disintegration into smaller fragments was observed. In the northern part of the Sredinny Range from 1950 to 2016–2017 glaciers decreased by 125 km<sup>2</sup> or 35.6%, and the rate of their reduction in the period from 2002 to 2016–2017 (1.45%/year) increased approximately 4.3 times compared to the period 1950–2002 (0.34%/year). The greatest reduction is observed in small glaciers with an area of less than 0.1 km<sup>2</sup> and in glaciers with southeastern and southern expositions. The main glacier area loss in this region occurred in the altitudinal zone of 1200–1800 m: 65.5 km<sup>2</sup> (25.2%) for the period from 2002 to 2016–2017. On the Kronotsky Peninsula, the glacier area reduction for 1957–2019 was 32.1 km<sup>2</sup> (35.6%), and the rates were almost the same in the years 1957–2000 (0.61%/year) and 2000–2019 (0.67%/year). The largest glacier area declines in this area for the period 2000–2019 occurred at altitudes below 500 m (55.1%) and 500–700 m (27.9%).

A slight increase in air temperature in summer (up to 0.3°C/10 years) and a decrease in precipitation in winter (on average 5%–10%/10 years) were revealed by weather station data and ERA5 reanalysis at Kamchatka Peninsula. At the same time, a significant increase in the radiation balance in May–September was found, along with a tendency in downward shortwave radiation increase for the last two decades due to a cloud amount decrease and mainly due to lower clouds. These trends are in good agreement with the geopotential height growth over the Kamchatka region for the last decades, as well as with the velocity divergence increase in the middle troposphere and the intensification of downward air movements. All this indicates a frequency of anticyclones increase over the region in the warm season, which,

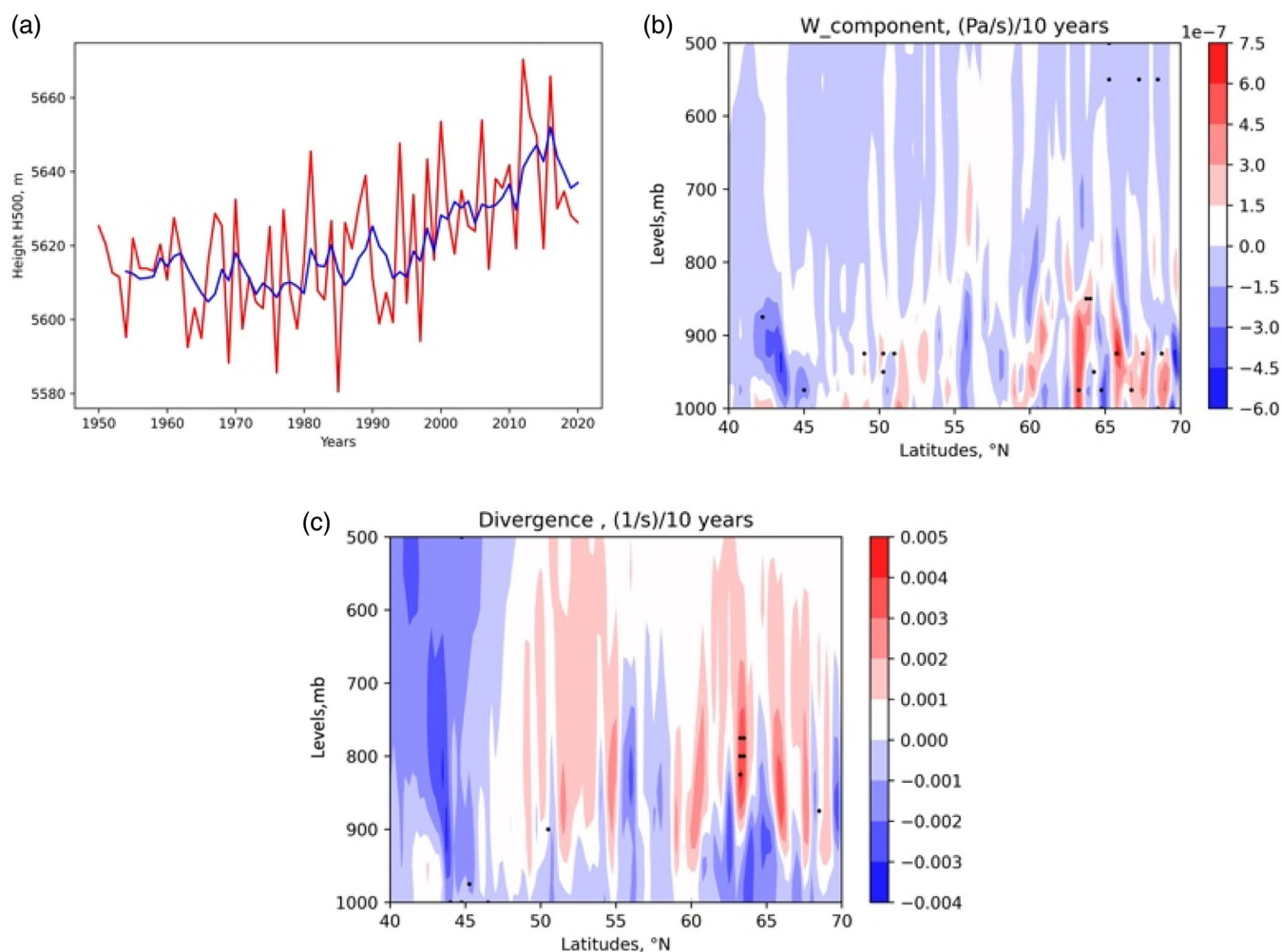


**FIGURE 12** The time series of geopotential height at 500 mb level on average for May–September and on average for the area 40–60 N 155–165 E (a, black line – 5 years moving averages); the transect of linear trend coefficients of vertical velocity (b) and velocity divergence (c) in average for May–September and in average for the longitudes 155–165 N. [Colour figure can be viewed at [wileyonlinelibrary.com](https://onlinelibrary.wiley.com)]

apparently, caused a radiation balance positive anomaly and, consequently, ablation, which, according to rough estimates, in the period 2010–2020 could be 25% higher than at the end of XX century. This is probably a consequence of the so-called ‘expansion of the tropics’ due to the expansion of the Hadley cell to the north, which in this region is manifested in the extending of the North Pacific High.

A positive radiation balance trend of 5 W/m<sup>2</sup>/10 years per season which causes an increase in the ablation layer of 60 mm/10 years, combined with a decrease in winter precipitation, gives an average mass balance trend of –12 mm·year<sup>–1</sup>. Modelling the evolution of typical glaciers of the Sredinny Range and the Kronotsky Peninsula using the minimal Oerlemans model gave reasonable estimates of the area reduction: –22% and –11% correspondingly, which is consistent with the observational data.

## AUTHOR CONTRIBUTIONS

**I. A. Korneva:** Methodology; investigation; formal analysis; visualization; project administration; writing – original draft; writing – review and editing. **P. A. Toropov:** Conceptualization; methodology; validation; supervision; writing – original draft; writing – review and editing. **A. Ya. Muraviev:** Data curation; methodology; investigation; formal analysis; writing – original draft. **M. A. Ale-shina:** Data curation.

## ACKNOWLEDGEMENTS

The climatic part of the study was carried out within the framework of the Russian Science Foundation (Grant No. 22-17-00159), the study of glaciation changes in the northern part of the Sredinny Range and the Kronotsky Peninsula was carried out within the framework of the research project FMGE-2019-0004 of the Research Plan of the Institute of Geography RAS.

## DATA AVAILABILITY STATEMENT

The data that support the findings of this study are available from the corresponding author upon reasonable request.

## ORCID

I. A. Korneva  <https://orcid.org/0000-0002-6453-8315>

P. A. Toropov  <https://orcid.org/0000-0003-0922-1486>

A. Ya. Muraviev  <https://orcid.org/0000-0001-9763-527X>

M. A. Aleshina  <https://orcid.org/0000-0001-8416-7657>

## REFERENCES

- A report on climate features on the territory of the Russian Federation in 2021. (2022) Moscow: Russian Federal Service for Hydrometeorology and Environmental Monitoring (Roshydromet), 104 p. [in Russian].
- Bokuchava, D.D. & Semenov, V.A. (2021) Mechanisms of the early 20th century warming in the Arctic. *Earth-Science Reviews*, 222, 103820. Available from: <https://doi.org/10.1016/j.earscirev.2021.103820>
- Bulygina, O.N., Razuvaev, V.N. & Aleksandrova, T.M. (2014a) *Description of daily air temperature and precipitation data at meteorological stations of Russia and Former USSR (TTTR)*. Certificate of state registration of the database no. 2014620942. Available from: <http://meteo.ru/data/162-temperature-precipitation#описание-массива-данных> [Accessed 10th July 2022].
- Bulygina, O.N., Razuvaev, V.N. & Aleksandrova, T.M. (2014b) *Description of the snow data at meteorological stations in Russia and the former USSR*. Certificate of state registration of the database no. 2014621201. Available from: <http://meteo.ru/data/165-snow-cover#описание-массива-данных> [Accessed 15th September 2022].
- Bulygina, O.N., Veselov, V.M. & Razuvaev, V.N. (2014c) *Description of the dataset of main meteorological parameters by terms at Russian stations*. Certificate of state registration of the database no. 2014620549. Available from: <http://meteo.ru/data/163-basic-parameters#описание-массива-данных> [Accessed 10th October 2022].
- Chen, J., del Genio, A.D., Carlson, B.E. & Bosilovich, M.G. (2008) The spatiotemporal structure of twentieth century climate variations in observations and reanalyses. Pt. I: long term trend. *Journal of Climate*, 21, 2611–2633.
- Chernokulsky, A.V., Bulygina, O.N. & Mokhov, I.I. (2011) Recent variations of cloudiness over Russia from surface daytime observations. *Environmental Research Letters*, 6(3), 035202. Available from: <https://doi.org/10.1088/1748-9326/6/3/035202>
- Di Mauro, B., Garzonio, R., Rossini, M., Filippa, G., Pogliotti, P., Galvagno, M. et al. (2019) Saharan dust events in the European Alps: role in snowmelt and geochemical characterization. *The Cryosphere*, 13(4), 1147–1165. Available from: <https://doi.org/10.5194/tc-13-1147-2019>
- Dumont, M., Tuzet, F., Gascoin, S., Picard, G., Kutuzov, S., Lafaysse, M. et al. (2020) Accelerated snow melt in the Russian Caucasus mountains after the Saharan dust outbreak in March 2018. *Journal of Geophysical Research: Earth Surface*, 125, e2020JF005641. Available from: <https://doi.org/10.1029/2020JF005641>
- Elvidge, A.D., Munneke, P.K., King, J.C., Renfrew, I.A. & Gilbert, E. (2020) Atmospheric drivers of melt on Larsen C ice shelf: surface energy budget regimes and the impact of foehn. *Journal of Geophysical Research: Atmospheres*, 125, e2020JD032463. Available from: <https://doi.org/10.1029/2020JD032463>
- ERA5: data documentation [homepage on the internet]. Available from: <https://confluence.ecmwf.int/display/CKB/ERA5%3A+data+documentation#ERA5:datadocumentation-References> [Accessed 25th February 2023].
- Fedotov, S.A. & Masurenkov, Y.P. (1991) *Active volcanoes of Kamchatka*. Moscow: Nauka, 302 p.
- Fukumoto, S., Sugiyama, S., Hata, S., Saito, J., Shiraiwa, T. & Mitsudera, H. (2023) Glacier mass change on the Kamchatka peninsula, Russia, from 2000 to 2016. *Journal of Glaciology*, 69 (274), 237–250. Available from: <https://doi.org/10.1017/jog.2022.50>
- Gandin, L.S. & Kagan, R.L. (1976) *Statistical methods interpretation of meteorological data*. Leningrad: Hydrometeoizdat, p. 280.
- Gilbert, A. & Vincent, C. (2013) Atmospheric temperature changes over the 20th century at very high elevations in the European Alps from englacial temperatures. *Geophysical Research Letters*, 40, 2102–2108.
- Genot, P., Dumont, M., Lim, S., Patris, N., Taupin, J.-D., Wagnon, P. et al. (2014) A 10 year record of black carbon and dust from a mera peak ice core (Nepal): variability and potential impact on melting of Himalayan glaciers. *The Cryosphere*, 8(4), 1479–1496. Available from: <https://doi.org/10.5194/tc-8-1479-2014>
- Glaciers-of-russia-english/main-page [homepage on the internet]. Available from: <https://sites.google.com/view/glaciers-of-russia-english/main-page> [Accessed 20th June 2022].
- Glazyrin, G.E., Muraviev, Y.D. & Vinogradov, V.N. (1985) About the climatic context of Kamchatka glaciation. *Glyaciologicheskie issledovaniya*. No 27. M.: Nauka, pp. 51–66 [in Russian].
- Gruza, G.V. & Rankova, E.Y. (2012) *Observed and expected climate changes over Russia: surface air temperature*. Obninsk: FGBU “VNIIGMI-MCD”, 194 s.
- Hock, R., Rasul, G., Adler, C., Cáceres, B., Gruber, S., Hirabayashi, Y. et al. (2019) High mountain areas. In: H.-O. Pörtner, D.C. Roberts, V. Masson-Delmotte, P. Zhai, M. Tignor, E. Poloczanska, K. Mintenbeck, A. Alegria, M. Nicolai, A. Okem, J. Petzold, B. Rama, N.M. Weyer (eds.) *IPCC special report on the ocean and cryosphere in a changing climate*. Cambridge and New York, NY: Cambridge University Press, pp. 131–202. Available from: <https://doi.org/10.1017/9781009157964.004>
- IPCC. (2021) Climate change 2021: the physical science basis. In: Masson-Delmotte, V., Zhai, P., Pirani, A., Connors, S.L., Péan, C., Berger, S. et al. (Eds.) *Contribution of working group I to the sixth assessment report of the Intergovernmental Panel on Climate Change*. Cambridge and New York, NY: Cambridge University Press. Available from: <https://doi.org/10.1017/9781009157896>
- Ippolitov, I.I., Kabanov, M.V., Loginov, S.V., Podnebesnykh, N.V. & Kharyutkina, E.V. (2008) Variability of temperature behavior over the Asian territory of Russia in the period of global warming. *Journal of Siberian Federal University. Biology*, 4, 323–344.

- Isaev, A.A. (1988) *The statistics in meteorology and climatology*. Moscow: Moscow University Press, 248 p.
- Kamchatka Department for Hydrometeorology and Environmental Monitoring [homepage on the internet]. (2020) *Brief description of the climatic features of the Kamchatka Peninsula*. Available from: <http://kammeteo.ru/gms9.html> [Accessed 2nd May 2020].
- Khen, G.V., Ustinova, E.I. & Sorokin, Y.D. (2019a) Principal climate indices for the North Pacific: nature and history (a review). *Izvestiya TINRO*, 197(2), 166–181 [in Russian]. Available from: <https://doi.org/10.26428/1606-9919-2019-197-166-181>
- Khen, G.V., Ustinova, E.I. & Sorokin, Y.D. (2019b) Variability and interrelation of the basic climate indices for the North Pacific: trends, climate shifts, spectra, correlations. *Izvestiya TINRO*, 199, 163–178.
- Khromova, T., Nosenko, G., Nikitin, S., Muraviev, A., Popova, V., Chernova, L. et al. (2019) Changes in the mountain glaciers of continental Russia during the twentieth to twenty-first centuries. *Regional Environmental Change*, 19(5), 1229–1247. Available from: <https://doi.org/10.1007/s10113-018-1446-z>
- Khromova, T.Y., Nosenko, G.A., Glazovsky, A.F., Muraviev, A.Y., Nikitin, S.A. & Lavrentiev, I.I. (2021) New inventory of the Russian glaciers based on satellite data (2016–2019). *Ice and Snow*, 61(3), 341–358. Available from: <https://doi.org/10.31857/S2076673421030093>
- Kiktev, D.B., Kruglova, E.N. & Kulikova, I.A. (2015) Large-scale modes of atmospheric variability. Part I. Statistical analysis and hydrodynamic modeling. *Russian Meteorology and Hydrology*, 40, 147–159. Available from: <https://doi.org/10.3103/S1068373915030012>
- Kim, H.-K., Moon, B.-K., Kim, M.-K., Park, J.-Y. & Hyun, Y.-K. (2021) Three distinct atmospheric circulation patterns associated with high temperature extremes in South Korea. *Scientific Reports*, 11(1). Available from: <https://doi.org/10.1038/s41598-021-92368-9>
- Kondratyuk, V.I. (1974) Climate of the Kamchatka Peninsula. In: *Moscow: Hydrometeoizdat*. Hydrometeoizdat: Moscow, p. 202.
- Kotlyakov, V. M., & Kravtsova, V. I. (1997) World atlas of snow and ice resources. (1997), Vol. 1. Moscow: Russian Academy of Sciences, 392 p.
- Lozhkin, D.M. & Shevchenko, G.V. (2021) Seasonal variability of sea level pressure in the Russian Far East. *Current Problems in Remote Sensing of the Earth from Space*, 18(4), 249–260.
- Lu, J., Vecchi, G.A. & Reichler, T. (2007) Expansion of the Hadley cell under global warming. *Geophysical Research Letters*, 34, L06805. Available from: <https://doi.org/10.1029/2006GL028443>
- Muraviev, A.Y. (2017) *Fluctuations in the glaciers of Kamchatka in the second half of the XX – the beginning of the XXI century*. PhD Thesis. Moscow: Institute of Geography RAS, 168 p. Available from: <http://igras.ru/sites/default/files/announcements/%D0%A2%D0%B5%D0%BA%D1%81%D1%82%20%D0%B4%D0%B8%D1%81%D1%81%D0%B5%D1%80%D1%82%D0%B0%D1%86%D0%B8%D0%B8.pdf> [Accessed 22 March 2023].
- Muraviev, A.Y. (2020a) Degradation of glaciers in the northern part of the Middle Range on Kamchatka peninsula along the period from 1950 over 2016–2017. *Ice and Snow*, 60(4), 498–512. Available from: <https://doi.org/10.31857/S2076673420040055>
- Muraviev, A.Y. (2020b) Distribution and morphology of present-day glaciers on Kamchatka. *Ice and Snow*, 60(3), 325–342. Available from: <https://doi.org/10.31857/S2076673420030043>
- Muraviev, A.Y. & Muraviev, Y.D. (2016) Fluctuations of glaciers of the Klyuchevskaya group of volcanoes in the 20th–21st centuries. *Ice and Snow*, 56(4), 480–492. Available from: <https://doi.org/10.15356/2076-6734-2016-4>
- Muraviev, A.Y. & Nosenko, G.A. (2013) Glaciation change in the northern part of the Middle Range on the Kamchatka peninsula in the second half of the XX century. *Ice and Snow*, 53(2), 5–11. Available from: <https://doi.org/10.15356/2076-6734-2013-2-5-11>
- Muravyev, Y.D., Shiraiwa, T., Yamaguchi, S., Matsumoto, T., Nishimura, K., Koshima, S. et al. (1999) Mass balance of glacier in condition of maritime climate – Koryto glacier in Kamchatka, Russia. In: *Cryospheric studies in Kamchatka*, Vol. II. Sapporo: Institute of Low Temperature Science Hokkaido University, pp. 51–61.
- NASA/METI/AIST/Japan Space Systems & U.S./Japan ASTER Science Team. (2018) *ASTER Global Digital Elevation Model V003*. Distributed by NASA EOSDIS Land Processes DAAC. Available from: <https://doi.org/10.5067/ASTER/ASTGTM.003>
- Norris, J.R. & Wild, M. (2007) Trends in aerosol radiative effects over Europe inferred from observed cloud cover, solar “dimming,” and solar “brightening”. *Journal of Geophysical Research: Atmospheres*, 112, D08214. Available from: <https://doi.org/10.1029/2006JD007794>
- Oerlemans, J. (2008) *Minimal glacier models*. Utrecht: Igitur, 91 p.
- Ohmura, A. (2001) Physical basis for the temperature-based melt-index method. *Journal of Applied Meteorology and Climatology*, 40(4), 753–761. Available from: [https://doi.org/10.1175/1520-0450\(2001\)040<0753:PBFTTB>2.0.CO;2](https://doi.org/10.1175/1520-0450(2001)040<0753:PBFTTB>2.0.CO;2)
- Pepin, N.C., Arnone, E., Gobiet, A., Haslinger, K., Kotlarski, S., Notarnicola, C. et al. (2022) Climate changes and their Elevational patterns in the mountains of the world. *Reviews of Geophysics*, 60(1), Portico. Available from: <https://doi.org/10.1029/2020rg000730>
- Philipona, R. (2013) Greenhouse warming and solar brightening in and around the Alps. *International Journal of Climatology*, 33(6), 1530–1537. Available from: <https://doi.org/10.1002/joc.3531>
- Philipona, R., Behrens, K. & Ruckstuhl, C. (2009) How declining aerosols and rising greenhouse gases forced rapid warming in Europe since the 1980s. *Geophysical Research Letters*, 36, L02806. Available from: <https://doi.org/10.1029/2008GL036350>
- Philipona, R., Dürr, B., Ohmura, A. & Ruckstuhl, C. (2005) Anthropogenic greenhouse forcing and strong water vapour feedback increase temperature in Europe. *Geophysical Research Letters*, 32, L19809. Available from: <https://doi.org/10.1029/2005GL023624>
- Porter, C., Morin, P., Howat, I., Noh, M.-J., Bates, B., Peterman, K. et al. (2018) «ArcticDEM», Harvard Dataverse, V1. Available from: <https://doi.org/10.7910/DVN/OHHUKH>. Archive of data from 29.08.2018–30.08.2018, 23.06.2020.
- Raup, B. & Khalsa, S.J.S. (2010) *GLIMS data analysis tutorial*. 15 p. Available from: [http://www.glims.org/MapsAndDocs/assets/GLIMS\\_Analysis\\_Tutorial\\_a4.pdf](http://www.glims.org/MapsAndDocs/assets/GLIMS_Analysis_Tutorial_a4.pdf) [Accessed 13 February 2022].
- RGI Consortium. (2017) *Randolph Glacier Inventory – a dataset of global glacier outlines: version 6.0: technical report, global land ice measurements from space*, Colorado, USA. Digital Media. Available from: <https://doi.org/10.7265/N5-RGI-60>
- RIHMI-WDC. *Baseline climatological data sets* [homepage on the internet]. Available from: [http://meteo.ru/english/climate/cl\\_data.php](http://meteo.ru/english/climate/cl_data.php) [Accessed 05 June 2022].



- Rottler, E., Kormann, C., Francke, T. & Bronstert, A. (2019) Elevation-dependent warming in the Swiss Alps 1981–2017: features, forcings and feedbacks. *International Journal of Climatology*, 39, 2556–2568. Available from: <https://doi.org/10.1002/joc.5970>
- Seager, R., Ting, M., Held, I., Kushnir, Y., Lu, J., Vecchi, G. et al. (2007) Model projections of an imminent transition to a more arid climate in southwestern North America. *Science*, 316(5828), 1181–1184.
- SENTINEL 2 Data Quality Report. (2020) ESA. Ref. S2-PDGS-MPC-DQR. Is. 51. 50 p. Available from: [https://sentinel.esa.int/documents/247904/685211/Sentinel-2\\_L1C\\_Data\\_Quality\\_Report](https://sentinel.esa.int/documents/247904/685211/Sentinel-2_L1C_Data_Quality_Report) [Accessed 10 May 2022].
- Shatilina, T.A. & Anzhina, G.I. (2008) Features of atmospheric circulation and climate in the Far East in the beginning of 21 century. *Izvestiya TINRO*, 152, 225–239.
- Sherwood, S.C., Meyer, C.L. & Allen, R.J. (2008) Robust tropo-spheric warming revealed by iteratively homogenized radiosonde data. *Journal of Climate*, 21, 5336–5350.
- Shestakova, A.A., Chechin, D.G., Lüpkes, C., Hartmann, J. & Maturilli, M. (2022) The foehn effect during easterly flow over svalbard. *Atmospheric Chemistry and Physics*, 22(2), 1529–1548.
- Shkaberda, O.A. (2015) *The modern tendencies of Kamchatka climate change*. PhD Thesis. Kazan, 235 p. [in Russian].
- Shkaberda, O.A. & Vasilevskaya, L.N. (2014) Long-term variability of the temperature and humidity regime on the Kamchatka peninsula. *Izvestiya TINRO*, 178(3), 217–233. Available from: <https://doi.org/10.26428/1606-9919-2014-178-217-233>
- Staten, P.W., Lu, J., Grise, K.M., Davis, S.M. & Birner, T. (2018) Re-examining tropical expansion. *Nature Climatic Change*, 8, 768–775. Available from: [10.1038/s41558-018-0246-2](https://doi.org/10.1038/s41558-018-0246-2)
- Tielidze, L.G. & Wheate, R.D. (2018) The Greater Caucasus glacier inventory. *The Cryosphere*, 12, 81–94. Available from: [10.5194/tc-12-81-2018](https://doi.org/10.5194/tc-12-81-2018)
- Toropov, P.A., Aleshina, M.A. & Grachev, A.M. (2019) Large-scale climatic factors driving glacier recession in the Greater Caucasus, 20th–21st century. *International Journal of Climatology*, 39, 4703–4720.
- Toropov, P.A., Debol'skii, A.V., Polyukhov, A.A., Shestakova, A.A., Popovnin, V.V. & Drozdov, E.D. (2023) Oerlemans minimal model as a possible instrument for describing mountain glaciation in earth system models. *Water Resources*, 50(5), 675–687.
- Vinogradov, V.N. (1968) *USSR Glacier Inventory*, Vol. 20. Parts 2–4. Leningrad: Hydrometeoizdat, 76 p.
- Vinogradov, V.N. & Ogorodov, N.V. (1966) Volcanoes and glaciers northern part of the Central Range. *Geographical Issues of Kamchatka*, 4, 70–85.
- Vuille, M. & Bradley, R. (2000) Mean annual temperature trends and their vertical structure in the tropical Andes. *Geophysical Research Letters*, 27(23), 3885–3888.
- You, Q., Kang, S., Pepin, N., Flügel, W.A., Yan, Y., Behrawan, H. et al. (2010) Relationship between temperature trend magnitude, elevation and mean temperature in the Tibetan Plateau from homogenized surface stations and reanalysis data. *Global and Planetary Change*, 71, 124–133.

**How to cite this article:** Korneva, I. A., Toropov, P. A., Muraviev, A. Y., & Aleshina, M. A. (2024). Climatic factors affecting Kamchatka glacier recession. *International Journal of Climatology*, 1–25. <https://doi.org/10.1002/joc.8328>